J. Phase Equilib. Diffus. (2022) 43:554–575
https://doi.org/10.1007/s11669-022-00999-w

Phase Equilibria in the Ti-Rich Part of the Ti-Al-Nb System—Part II: High-Temperature Phase Equilibria Between 1000 and 1300 °C

B. Distl[1] · K. Hauschildt[2] · F. Pyczak[2] · F. Stein[1]

Submitted: 22 June 2022 / in revised form: 19 July 2022 / Accepted: 10 August 2022 / Published online: 8 November 2022

Abstract The knowledge of phase equilibria in the Ti-Al-Nb system above 1000 °C is of importance for the manufacturing of TiAl-based parts for high-temperature structural applications. Especially the extended homogeneity range of the cubic (βTi,Nb) phase, which is determined by its Al solubility, and the position and extension of the high-temperature (αTi) phase is of crucial importance for the hot-workability and microstructure control of these alloys. However, the phase diagrams reported in the literature are very contradicting especially regarding these aspects. For this reason, a systematic reinvestigation of the phase equilibria in this part of the system was carried out. A total of 17 ternary alloys were synthesized, heat-treated at 1000-1300 °C, and analyzed by electron probe microanalysis (EPMA), x-ray diffraction (XRD), high-energy XRD (HEXRD), and differential thermal analysis (DTA) to determine composition and type of equilibrium phases as well as transition temperatures. With this information, isothermal sections of the Ti-rich part of the Ti-Al-Nb system at 1000, 1100, 1200, and 1300 °C were established. An isolated $(\beta\text{Ti,Nb})_o$ phase field is found to be stable at 1000 and 1100 °C. Furthermore, the formation and homogeneity range of (αTi) at high temperatures as well as the presence of Ti_3Al at 1200 °C is experimentally investigated and discussed. Based on the observed phase equilibria and transition temperatures, an improved reaction scheme for the entire Ti-Al-Nb system is proposed.

✉ B. Distl
distl@mpie.de

[1] Max-Planck-Institut Für Eisenforschung GmbH, Düsseldorf, Germany

[2] Helmholtz Zentrum Hereon, Geesthacht, Germany

Keywords experimental study · intermetallics · isothermal section · ternary phase diagram

1 Introduction

One of the main challenges in manufacturing TiAl-based parts for high-temperature structural applications is the relatively low room temperature ductility of the respective alloys.[1] Complex processing routes are required to manufacture parts from such materials.[2-5] In addition, homogeneous, isotropic mechanical properties, which can be achieved by controlling texture and microstructure, are prerequisite to use these alloys as structural materials at high temperatures. To achieve this, the respective alloy must meet certain requirements: (1) no significant texture after casting; (2) minimal amount of peritectically solidified (αTi); (3) good deformability during thermomechanical treatment; (4) thermomechanical treatment not performed in single-phase (αTi) field; (5) certain volume fraction ratio between the intermetallic phases TiAl and Ti_3Al in the microstructure; (6) thermally stable microstructure.[4] A promising approach to achieve these requirements is based on the addition of so-called β-stabilizing elements (e.g. Nb, Mo). The bcc metals Nb and Mo both form solid solutions with bcc (βTi) with complete miscibility at high temperatures, which is why the solid solution phases in the binary (and higher component) systems are written as (βTi,Nb) or (βTi,Mo). From the viewpoint of the binary Ti-Al system, additions of Nb to (βTi) extend the single-phase field to higher Al contents compared to the binary Ti-Al system.[6] This changes the solidification sequence from L (liquid phase) → L + (βTi,Nb) → (αTi) → … to L → L + (βTi,Nb) →

(βTi,Nb) →… for certain composition regions (e.g., 42-48 at.% Al) and results in a smaller amount of the peritectically solidified (αTi) and a more equiaxed and lamellar microstructure at room temperature.[7] The shift of the (βTi,Nb) phase field to higher Al contents has additional advantages: (1) the hot-working temperature is lowered[5]; (2) hot-working can be performed in the two-phase field (βTi,Nb) + (αTi) by avoiding the single-phase (αTi) phase field, and (3) the phase fraction of (αTi)/Ti_3Al is increased during hot working and heat treatment[4] (Fig. 1). The above-mentioned facts make the approach of alloying β-stabilizing elements to TiAl-based alloys suitable to meet the alloy design requirements and facilitate further improvements and the development of such alloys. However, a prerequisite for developing respective alloys is a very precise knowledge of phase equilibria at different temperatures and compositions.[4]

In the temperature range studied here, several isothermal sections have been published, some of these cover the entire compositional range of the ternary Ti-Al-Nb system.[9-17] However, the data are often very contradicting. As an example, Fig. 2 shows experimental data from three different studies[11,14,18] in the composition range between 0 and 60 at.% Al and 0 to 50 at.% Nb for 1100 °C[10], which includes all relevant phases for currently used TiAl-based alloy. As can be seen, Li et al.[11] (grey lines and symbols) report a Ti_3Al + TiAl + Nb_2Al tie-triangle whereas the experimental data from Eckert et al.[14] (red) and data summarized by Kattner and Boettinger[18] (blue) show the presence of two different three-phase equilibria ((βTi,Nb)$_o$ + TiAl + Nb_2Al and (βTi,Nb)$_o$ + Ti_3Al + TiAl). Furthermore, the tie-lines reported for the two-phase field (βTi,Nb) + Ti_3Al show completely different inclinations and intersect each other (Fig. 2), which shows the need for further investigations to clear up these contradictions and to investigate the possible presence of the tie-triangle (βTi,Nb)$_o$ + Ti_3Al + Nb_2Al reported by Li et al.[11] Similar observations are also made at other temperatures.

In another study covering 1100 °C, Chen et al.[10] reported a new ternary intermetallic compound, which was named γ_1 ($TiAl_3Nb$) as it was claimed to be a kind of superstructure of TiAl. The existence of this phase is controversial and has been discussed at length.[19-21] Since other studies[11,13,19] have not been able to reproduce these results when employing similar experimental procedures as described in Ref. 10, it is not considered an equilibrium phase in more recent assessments.[22-24]

Another difference in the reported phase equilibria relates to the homogeneity range of Ti_3Al at 1200 °C: According to the binary Ti-Al phase diagram[8,25] Ti_3Al is formed peritectoidally from (αTi) and (βTi) just at 1200 °C, and therefore, its phase field—if anyone exists in the ternary—should only be connected to the boundary system at one composition (~ 32 at.% Al). Hellwig et al.[13] reported an isothermal section at 1200 °C based on diffusion couple experiments and equilibrated bulk alloys, showing a Ti_3Al phase field extending from 30 to 33 at. % Al along the binary Ti-Al axis and up to 10 at.% Nb into the ternary composition triangle. In contrast to this, Takeyama et al.[26] suggested the existence of an isolated Ti_3Al phase field in the ternary composition triangle, and Kainuma et al.[15] did not report Ti_3Al to be stable at 1200 °C. Similar disagreement exists with respect to the extension of the (αTi) phase field at high temperatures. In a

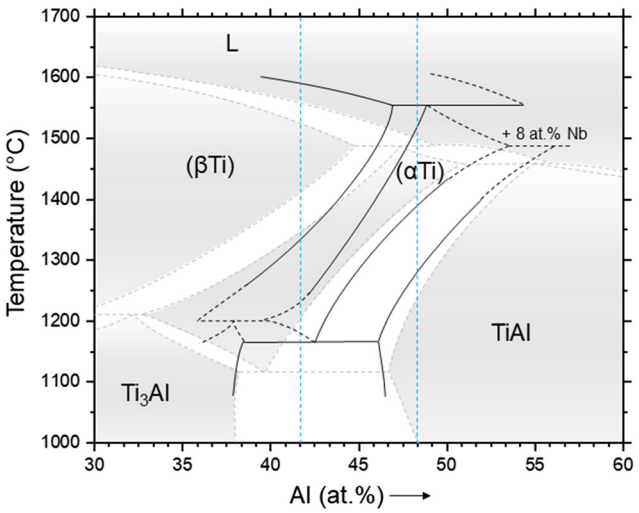

Fig. 1 Binary Ti-Al phase diagram[8] overlaid with the experimental data from Chen et al.[6] (black lines, addition of 8 at.% Nb) showing the changes to the phase fields in the application relevant composition range (blue lines) described in the text above

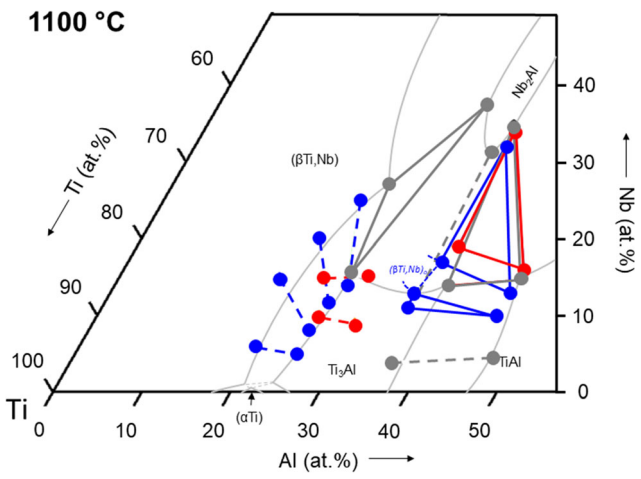

Fig. 2 Isothermal section at 1100 °C from Li et al.[11] (grey dots and lines) superimposed with experimental results from Eckert et al.[14] (red dots and lines) and summarized results by Kattner and Boettinger[18] (blue dots and lines) showing several contradicting phase equilibria (Color figure online)

recent experimental study by Xu et al. (Ref 9) on phase equilibria at 1300 °C, a Nb solubility of 16.0 at.% was measured in (αTi), whereas in some earlier studies values of 11.1[15,27] and 12.5 at.% Nb[15,27] were reported for the same temperature. There is also not much information available on the stability range of (βTi,Nb)$_o$ at temperatures above 1000 °C.

Several thermodynamic descriptions of the Ti-Al-Nb system are available.[18,23,24,28,29] However, as they are of course always based on the experimental results available at the time, they do not agree very well. Even the more recent descriptions presented by Witusiewicz et al.[24] and Cupid et al.[23], which considered new data at that time especially in the composition range Ti-(40-50) Al-(2-10) Nb,[13,15,16,20,30-33] do not allow a satisfactory description of the experimental phase equilibria as shown exemplarily by Witusiewicz et al. for 1000 °C (c.f. Figure 3 in Ref. 24).

The inconsistencies described above and the fact that data are still simply missing in various composition and temperature ranges show that the currently available experimental data and thermodynamic descriptions are not sufficient to reliably predict the phase equilibria in the system. Therefore, a series of heat-treated bulk alloys (10-45 at.% Al and 5-25 at.% Nb) were investigated after heat treatment between 1000 and 1300 °C in the present work. Partial isothermal sections are constructed based on the analysis of the results obtained by scanning electron microscopy (SEM), electron probe microanalysis (EPMA), x-ray diffraction (XRD), high-energy XRD (HEXRD), and differential thermal analysis (DTA). Phase equilibria at lower temperatures from 700 to 900 °C were already discussed and presented in Part I of this study.[34] Based on the combined experimental results which thus cover the temperature range from 700 to 1300 °C and considering some information from the literature especially regarding still higher temperatures, a complete reaction scheme of the Ti-Al-Nb system is presented in the last section.

2 Experimental

For the present investigation of phase equilibria between 1000 and 1300 °C, a series of 17 ternary alloys (Table 1 and Fig. 3) was synthesized in an arc melter with a tiltable crucible. The synthesis was performed in Ar atmosphere, which was additionally dried (ZPure M^{TM} 3800 cc, Chromatography research supplies) to remove residual moisture and oxygen. High-purity elements Ti (99.995 wt.%), Al (99.999 wt.%), and Nb (99.9 wt.%) (HMW Hauner GmbH & Co. KG) were used for the synthesis of rod-shaped alloys (15 mm in diameter, 160 mm in length) weighing between 200 and 300 g (depending on composition). The overall composition and impurity

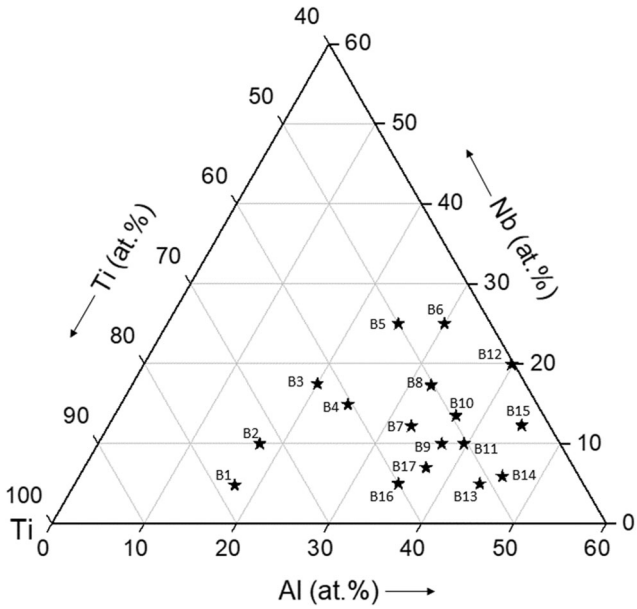

Fig. 3 Alloy compositions of the ternary bulk alloys B1-B17

content were determined for selected as-cast and heat-treated alloys using inductively coupled plasma atomic emission spectroscopy (ICP-AES, Optima 8300, Perkin Elmer) and inert gas fusion (Fusionmaster ONH, NCS Germany).

To minimize the uptake of impurities during heat treatment, two different setups were used depending on the heat treatment temperature: (1) encapsulation in fused silica ampoules for heat treatments at 1000 and 1100 °C; (2) a so-called "double crucible technique" above 1100 °C.[35] Cylinders with a length of 10 mm were cut from the as-cast alloys and encapsulated in fused silica ampules that were backfilled with Ti gettered Ar gas for heat treatments at 1000 and 1100°. At temperatures above 1100 °C, the fused silica is no longer sufficiently gas-tight for oxygen and nitrogen[36] causing the initiation of the devitrification process. Therefore, a double crucible technique[35] is used for heat treatments at 1200 and 1300 °C. The sample is wrapped with Ta foil and placed in an alumina crucible, which in turn is placed upside down in a larger crucible. The leftover space is filled with Ti filings which act as getter material. The Ta foil prevents contact between filings and the sample. Additionally, the reaction between Ta and the sample is very sluggish, so Ta was not found in any of the samples. In both cases the samples were quenched in brine by breaking the ampules/crucibles. The described schematic setup of the heat treatment methods is shown in Fig. 4.

For selected alloys, the overall composition (measured by EPMA) and the content of O and N after heat treatment were checked. The change in overall composition was within the measurement uncertainty of ± 1%[37] for the

Table 1 Synthesized ternary alloys B1 to B17 with their nominal and measured compositions (ICP-AES) as well as their impurity contents (O, N, C). For N, the values were below the detection limit of 50 wt. ppm and therefore are not listed here

No	Nominal composition, at.%			Measured as-cast composition (ICP-AES), at.%			Impurity contents, wt. ppm		Heat treatment time, h			
	Ti	Al	Nb	Ti	Al	Nb	O	C	1000 °C	1100 °C	1200 °C	1300 °C
B1	77.5	17.5	5	77.8	17.4	4.8	290	130	400	200		
B2	72.5	17.5	10						400	200		
B3	62.5	20	17.5				220		400	200		
B4	60	25	15	60.5	24.6	14.9	130	110	400	200		
B5	50	25	25						650	400	30	20
B6	45	30	25						650	400	30	20
B7	54.5	33	12.5	55	32.8	12.2	180	85	400	200		
B8	49	33	17.5	50.3	32.4	17.3	290	120	400	200	30	20
B9	53	37	10	52.8	37.2	10.0	160	86	400	200	30	20
B10	49.5	37	13.5						400	200	30	
B11	50	40	10	50.4	39.6	10.0	290	160	400	200	30	20
B12	40	40	20	40.3	39.8	19.9	130	110	400	200	30	20
B13	50	45	5	50.7	43.4	4.9	150	108	400	200	30	20
B14	47.5	45	7.5	48.3	45.8	5.9	140	89	400	200	30	20
B15	42.5	45	12.5	43.0	44.7	12.3	200	102	400	200	30	20
B16	60	35	5							400	30	
B17	56	37	7								30	

The heat treatment times at 1000, 1100, 1200 and 1300 °C are given in the last columns

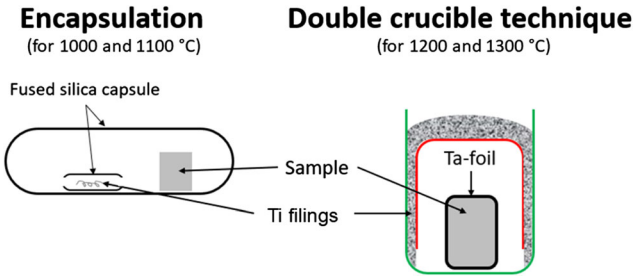

Fig. 4 Schematic heat treatment setups: encapsulation of samples for 1000 and 1100 °C and applying the 'double crucible technique' for temperatures of 1200 and 1300 °C

EPMA measurement. The nitrogen content remained below 50 wt. ppm (detection limit) and the oxygen content increased only slightly.

The phase compositions were determined by EPMA (JEOL JXA-8100) operated at an acceleration voltage of 15 kV, a probe current of 20 nA, and pure elements as standard. Overall and phase compositions were determined as described in Ref. 34. Furthermore, the experimental details for phase identification by room temperature XRD and HEXRD, in situ HEXRD as well as the measurement of phase transformation temperatures investigated by DTA were carried out as described in Ref. 34.

3 Results

The determined phase and alloy compositions, phase fractions, and lattice parameters measured after the different heat treatments are summarized in Tables 2, 3, 4 and 5. The alloy compositions given together with the alloy numbers in the following text always refer to the compositions measured in the as-cast condition (or, if not measured, to the nominal composition).

In the following, some characteristic microstructures of heat-treated alloys and the resulting phase equilibria are presented. The microstructure of alloy B1 (Ti-17.4Al-4.8Nb) at 1000 °C (Fig. 5a) consists of Ti_3Al (dark phase) and a (βTi,Nb) matrix. Two different contrasts in the (βTi,Nb) matrix are observed in the BSE image (Fig. 5b), but no variations in composition could be measured by EPMA. This is most likely due to a martensitic (i.e. non-equilibrium) transformation taking place during quenching from 1000 °C, which is a well-known effect occurring in this composition range (see, e.g., the assessment of Tretyachenko[22]). At 1100 °C, (βTi,Nb) is the only microstructure constituent. This is consistent with DTA measurements of this sample, which show that the continuous dissolution of Ti_3Al is finished at 1022 °C.

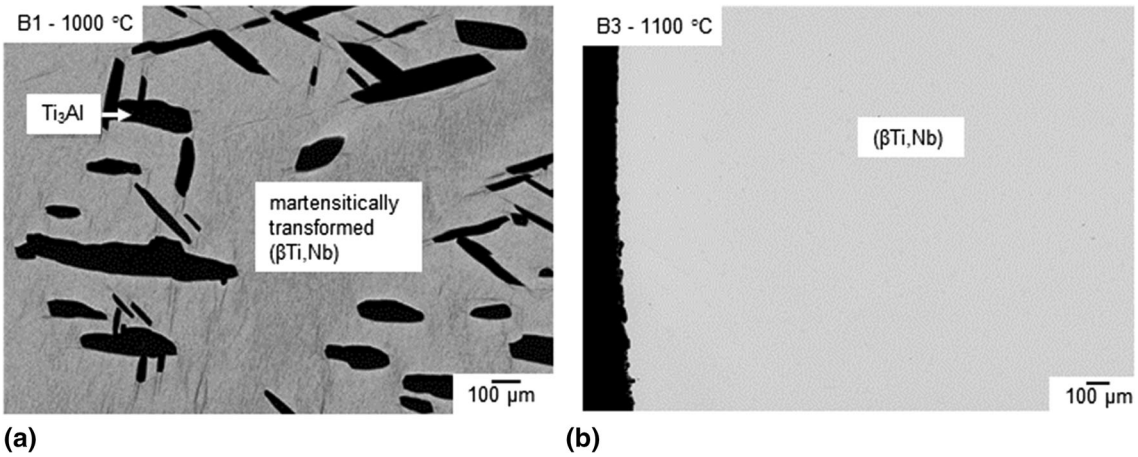

Fig. 5 Back-scattered electron (BSE) image of (a) alloy B1 (Ti-17.4Al-4.8Nb) quenched from 1000 °C showing a two-phase microstructure (Ti_3Al + (βTi,Nb)) and (b) alloy B3 (Ti-20-0Al-17.5Nb) quenched from 1100 °C being single-phase (βTi,Nb)

Alloys B2 (Ti-17.5Al-10.0Nb) and B3 (Ti-20.0Al-17.5Nb) are single-phase (βTi,Nb) at 1000 and 1100 °C, which is confirmed by DTA measurements. As can be seen in Fig. 6, the continuous dissolution of Ti_3Al ends at 995 (B2) and 985 °C (B3), whereupon the heat flow signal returns to the baseline.

In alloy B4 (Ti-24.6Al-14.9Nb), a two-phase microstructure consisting of *B*2-ordered (βTi,Nb) and Ti_3Al is observed in the sample quenched from 1000 °C (Fig. 7a). This is confirmed by HEXRD measurements of this sample (Fig. 7b) as well as in situ HEXRD measurements. The Ti_3Al phase formed predominantly at the grain boundaries of the (βTi,Nb) grains. At 1100 °C, this alloy is single-phase $(\beta Ti,Nb)_o$.

Alloy B5 (Ti-25.0Al-25.0Nb) shows a single-phase microstructure over the complete temperature range. The ordered $(\beta Ti,Nb)_o$ phase is present up to 1169 °C, while above this temperature the alloy is single-phase disordered (βTi,Nb) (alloy A11 in Ref. 38).

The three phases $(\beta Ti,Nb)_o$, Ti_3Al, and Nb_2Al are observed in the microstructure of alloy B6 (Ti-30.0Al-25.0Nb) quenched from 1000 °C (Fig. 7c), which is confirmed by HEXRD measurements (Fig. 7d). At 1100 and 1200 °C, the microstructure consists of a $(\beta Ti,Nb)_o$ matrix and Nb_2Al. At 1300 °C, only the *A*2-disordered (βTi,Nb) phase is present. In addition to the disordering taking place at 1243 °C (alloy A10 in Ref. 38), Nb_2Al dissolves completely above 1200 °C. Its phase fractions decreases from 26 vol.% at 1100 °C to only 3 vol.% at 1200 °C, i.e., the solvus temperature can be expected to be in the range from 1200 to ~ 1220 °C. However, the exact temperature could not be determined by the DTA measurements due to the slow, continuous decrease in phase fraction.

Alloy B7 (Ti-32.8Al-12.2Nb) shows a two-phase microstructure consisting of $(\beta Ti,Nb)_o$ and Ti_3Al at 1000 (Fig. 8a) and 1100 °C. The same two phases are observed in alloy B8 (Ti-32.4Al-17.3Nb) quenched from 1000 °C (Fig. 8b). At higher temperature this alloy is single-phase (βTi,Nb) with *B*2-ordering present up to 1248 °C (alloy A8 in Ref. 38).

Both alloys B9 (Ti-37.2Al-10.0Nb) and B11 (Ti-39.6Al-10.0Nb) show a three-phase microstructure composed of $(\beta Ti,Nb)_o$, Ti_3Al, and TiAl at 1000 and 1100 °C (Fig. 9a,b). For alloy B11, the in situ HEXRD measurements show that the transformation of Ti_3Al to (αTi) is finished at ~ 1175 °C (Fig. 10). This agrees with DTA measurements, which show that the transition takes place at 1171 °C. Therefore, at 1200 °C the equilibrium phases are (αTi), $(\beta Ti,Nb)_o$, and TiAl. Due to the dissolution of Ti_3Al and TiAl with increasing temperature and the disordering of $(\beta Ti,Nb)_o$, which is observed with DTA and in situ HEXRD measurements, both alloys are single-phase (βTi,Nb) at 1300 °C. Figure 9c shows the intensity of the (001) and (110) peaks of TiAl in alloy B9. A continuous decrease in intensity is observed up to about 1150 °C, which marks the dissolution temperature of TiAl. In the DTA measurements of alloy B9, a very shallow effect is observed in this temperature range, which agrees with the observations made by in situ HEXRD. The intensity of the (100) superstructure reflection of $(\beta Ti,Nb)_o$ shown in Fig. 9d vanishes at the disordering temperature of 1222 °C, which is the same value as obtained by DTA measurements (alloy A4 in Ref. 38).

$(\beta Ti,Nb)_o$ and TiAl are present in the microstructure of alloy B10 (Ti-37.0Al-13.5Nb) at 1000 and 1100 °C. Since DTA measurements show that the *B*2-ordering of (βTi,Nb) disappears above 1225 °C, the single-phase microstructure observed at 1200 °C must belong to $(\beta Ti,Nb)_o$.

The three-phase equilibrium $(\beta Ti,Nb)_o$ + TiAl + Nb_2Al is observed in alloy B12 (Ti-39.8Al-19.9Nb) at 1000

Table 2 EPMA and HEXRD results on phase contents, alloy and phase compositions, phase fractions and lattice parameters of alloys heat-treated at 1000 °C for the times given in Table 1 (accuracy of the lattice parameters is ± 0.001 Å, n.d.: not determined)

Alloy No	Composition after heat treatment, at.%	Phases	Phase composition measured with EPMA, at.%		Phase fraction, vol.%	Pearson symbol	Lattice parameters, Å	
			Al	Nb			a	c
B1	Ti-17.8Al-4.8Nb	(βTi,Nb)	17.7 ± 0.2	4.7 ± 0.1	96	*cI*2	n.d	
		Ti_3Al	23.0 ± 0.2	2.8 ± 0.1	4	*hP*8	n.d	n.d
B2[a]	Ti-17.6Al-10.1Nb	(βTi,Nb)	17.6 ± 0.1	10.1 ± 0.1	100	*cI*2	n.d	
B3[a]	Ti-19.7Al-17.7Nb	(βTi,Nb)	19.7 ± 0.1	17.7 ± 0.3	100	*cI*2	n.d	
B4	Ti-25.2Al-13.9Nb	$(\beta Ti,Nb)_o$	24.2 ± 0.1	16.3 ± 0.2	55	*cP*2	3.245	
		Ti_3Al	26.6 ± 02	11.0 ± 0.1	45	*hP*8	5.789	4.662
B5[a]	Ti-25.0Al-24.9Nb	$(\beta Ti,Nb)_o$	25.0 ± 0.2	24.9 ± 0.3	100	*cP*2	n.d	
B6	Ti-30.4Al-22.9Nb	$(\beta Ti,Nb)_o$	29.1 ± 0.2	20.1 ± 0.3	77[b]	*cP*2	3.236	
		Ti_3Al	28.2 ± 0.2	14.2 ± 0.2	8[b]	*hP*8	5.790	4.680
		Nb_2Al	32.5 ± 0.2	32.8 ± 0.6	15[b]	*tP*30	9.943	5.137
B7	Ti-32.8Al-12.2Nb	$(\beta Ti,Nb)_o$	33.3 ± 0.2	12.4 ± 0.3	84	*cP*2	3.226	
		Ti_3Al	32.3 ± 0.2	9.1 ± 0.3	16	*hP*8	5.778	4.656
B8	Ti-32.4Al-17.3Nb	$(\beta Ti,Nb)_o$	32.4 ± 0.1	17.2 ± 0.2	98	*cP*2	3.229	
		Ti_3Al	30.9 ± 0.1	12.3 ± 0.2	2	*hP*8	5.777	4.681
B9	Ti-37.2Al-10.0Nb	$(\beta Ti,Nb)_o$	35.8 ± 0.1	10.7 ± 0.1	64	*cP*2	3.223	
		Ti_3Al	36.2 ± 0.2	8.0 ± 0.1	32	*hP*8	5.774	4.644
		TiAl	45.3 ± 0.3	7.7 ± 0.1	5	*tP*4	4.030	4.061
B10[c]	Ti-36.7Al-12.9Nb	$(\beta Ti,Nb)_o$	34.9 ± 0.2	13.3 ± 0.1	81	*cP*2	3.223[d]	
		TiAl	44.6 ± 0.2	10.0 ± 0.2	19	*tP*4	4.035[d]	4.060
B11	Ti-39.1Al-9.5Nb	$(\beta Ti,Nb)_o$	35.5 ± 0.4	11.1 ± 0.2	46	*cP*2	n.d	
		Ti_3Al	36.0 ± 0.3	8.3 ± 0.2	17	*hP*8	n.d	n.d
		TiAl	44.9 ± 0.3	8.1 ± 0.2	36	*tP*4	n.d	n.d
B12[c]	Ti-40.2Al-19.1Nb	$(\beta Ti,Nb)_o$[e]	35.5 ± 1.0	17.5 ± 1.0	22	*cP*2	3.228[d]	
		TiAl	45.3 ± 0.4	13.6 ± 0.1	48	*tP*4	4.032[d]	4.074
		Nb_2Al	35.2 ± 0.4	29.9 ± 0.4	29	tP30	9.929[d]	5.134
B13[e]	Ti-43.7Al-5.3Nb	Ti_3Al	36.9 ± 0.6	5.4 ± 0.2	26	*hP*8	5.777	4.634
		TiAl	46.1 ± 0.4	5.0 ± 0.5	74	*tP*4	4.014	4.062
B14	Ti-45.8Al-5.9Nb	Ti_3Al	37.1 ± 0.3	6.0 ± 0.2	7	*hP*8	5.770	4.637
		TiAl	46.5 ± 0.3	5.6 ± 0.2	93	*tP*4	4.017	4.063
B15[c]	Ti-43.9Al-12.3	$(\beta Ti,Nb)_o$	35.3 ± 0.2	16.2 ± 0.3	16	*cP*2	3.225	
		TiAl	45.5 ± 0.2	11.9 ± 0.3	84	*tP*4	4.032	4.064

[a]DTA measurements (Fig. 6) show that this alloy is single-phase (βTi,Nb) at 1000 °C despite a small phase fractions of Ti_3Al observed in the microstructure

[b]Phase fractions determined by HEXRD measurement

[c]Alloy contains a small amount of Ti_3Al, which is not considered an equilibrium phase, see section 3 in Ref. 34

[d]Lattice parameters determined by XRD measurements

[e]Phase compositions determined based on tie-line data of alloy B15

and 1100 °C (Fig. 11a). The disordering temperature of (βTi,Nb) in this alloy lies at 1199 °C (alloy A9 in Ref. 38), therefore the three-phases observed at 1200 °C are (βTi,Nb), TiAl, and Nb_2Al (Fig. 11b). The phase fraction of $(\beta Ti,Nb)_o/(\beta Ti,Nb)$ has increased from 22 vol.% at 1000 and 25 vol.% at 1100 to 67 vol.% at 1200, and at 1300 °C the alloy is finally single-phase (βTi,Nb).

A two-phase microstructure is observed in alloys B13 (Ti-43.4Al-4.9Nb) and B14 (Ti-45.8Al-5.9Nb) over the entire temperature range (Fig. 12a-c). DTA measurements

Table 3 EPMA and HEXRD results on phase contents, alloy and phase compositions, phase fractions, and lattice parameters of alloys heat-treated at 1100 °C for the times given in Table 1 (accuracy of the lattice parameters is ± 0.001 Å, n.d.: not determined)

Alloy No	Composition after heat treatment, at.%	Phases	Phase composition measured with EPMA, at.%		Phase fraction, vol.%	Pearson symbol	Lattice parameters, Å	
			Al	Nb			a	c
B1	Ti-17.4Al-4.8Nb	(βTi,Nb)	17.4 ± 0.1	4.8 ± 0.1	100	*cI*2	n.d	
B2	Ti-18.4Al-9.6Nb	(βTi,Nb)	18.4 ± 0.1	9.6 ± 0.1	100	*cI*2	n.d	
B3	Ti-20.2Al-17.2Nb	(βTi,Nb)	20.2 ± 0.1	17.2 ± 0.1	100	*cI*2	n.d	
B4	Ti-24.1Al-14.5Nb	(βTi,Nb)$_o$	24.1 ± 0.1	14.5 ± 0.1	100	*cP*2	n.d	
B5	Ti-25.8Al-23.8Nb	(βTi,Nb)$_o$	25.8 ± 0.2	23.8 ± 0.2	100	*cP*2	n.d	
B6	Ti-30.9Al-24.8Nb	(βTi,Nb)$_o$	30.1 ± 0.2	21.4 ± 0.2	74	*cP*2	n.d	
		Nb_2Al	33.6 ± 0.1	34.0 ± 0.5	26	*tP*30	n.d	n.d
B7	Ti-33.4Al-11.5Nb	(βTi,Nb)$_o$	33.3 ± 0.2	11.7 ± 0.1	95	*cP*2	3.226	
		Ti_3Al	32.5 ± 0.2	8.8 ± 0.1	5	*hP*8	5.772	4.677
B8	Ti-32.3Al-16.6Nb	(βTi,Nb)$_o$	32.3 ± 0.3	16.6 ± 0.3	100	*cP*2	3.227[d]	
B9	Ti-37.2Al-10.0Nb[b]	(βTi,Nb)$_o$	36.9 ± 0.2	10.0 ± 0.2	72	*cP*2	3.219	
		Ti_3Al	38.1 ± 0.2	8.0 ± 0.2	26	*hP*8	5.767	4.640
		TiAl	45.7 ± 0.1	7.6 ± 0.2	2	*tP*4	4.027	4.057
B10[c]	Ti-37.0Al-13.5Nb[a]	(βTi,Nb)$_o$	36.4 ± 1.0	13.1 ± 1.0	n.d	*cP*2	n.d	
		TiAl	45.0 ± 1.0	10.2 ± 1.0	n.d	*tP*4	n.d	n.d
B11	Ti-40.3Al-9.3Nb	(βTi,Nb)$_o$	36.9 ± 0.2	10.5 ± 0.2	46	*cP*2	n.d	
		Ti_3Al	38.3 ± 0.2	8.4 ± 0.1	19	*hP*8	n.d	n.d
		TiAl	45.8 ± 0.4	8.2 ± 0.1	35	*tP*4	n.d	n.d
B12	Ti-41.2Al-18.0Nb	(βTi,Nb)$_o$	36.3 ± 0.2	17.0 ± 0.2	25	*cP*2	3.217[d]	
		TiAl	45.4 ± 0.3	13.6 ± 0.1	50	*tP*4	4.019[d]	4.060[d]
		Nb_2Al	35.9 ± 0.2	30.7 ± 0.3	21	*tP*30	9.899[d]	5.119[d]
B13	Ti-43.6Al-5.1Nb	Ti_3Al	37.8 ± 0.4	5.0 ± 0.2	22	*hP*8	5.765[d]	4.637[d]
		TiAl	45.3 ± 0.4	5.0 ± 0.2	78	*tP*4	4.014[d]	4.060[d]
B14	Ti-45.8Al-5.9Nb[b]	Ti_3Al	37.1 ± 0.3	5.8 ± 0.1	n.d	*hP*8	5.766	4.640
		TiAl	45.0 ± 0.2	5.9 ± 0.1	n.d	*tP*4	4.014	4.060
B15[c]	Ti-44.4Al-11.9Nb	(βTi,Nb)$_o$	36.1 ± 0.3	15.2 ± 0.2	8	*cP*2	3.224[d]	
		TiAl	45.0 ± 0.2	11.9 ± 0.3	92	*tP*4	4.022[d]	4.067[d]
B16	Ti-35.0Al-6.7Nb	(βTi,Nb)$_o$	35.1 ± 0.2	7.2 ± 0.3	66	*cP*2	n.d	
		Ti_3Al	35.3 ± 0.2	5.5 ± 1.0	34	*hP*8	n.d	n.d

[a]Nominal composition

[b]As-cast composition. Phase fractions from HEXRD since the as-cast composition lies outside the tie-triangle/tie-line

[c]Alloy contains a small amount of Ti_3Al, which is not considered an equilibrium phase, see Section 3 in Ref. 34

[d]Lattice parameters determined by XRD measurements

show, that the transformation from Ti_3Al to (αTi) takes place between 1100 and 1200 °C.[38] Therefore, the phases in equilibrium at and below 1100 °C are Ti_3Al and TiAl, while at 1200 °C the stable phases are (αTi) and TiAl. These phase equilibria have been confirmed by DTA, XRD and HEXRD measurements. From 1000 to 1200 °C, (βTi,Nb)$_o$ + TiAl are observed in the quenched samples of alloy B15 (Ti-44.7Al-12.3Nb). At 1300 °C, a three-phase microstructure consisting of (αTi), (βTi,Nb), and TiAl, was observed (Fig. 12d) and has been confirmed by HEXRD measurements.

Alloys B16 (Ti-35.0Al-5.0Nb) and B17 (Ti-37.0Al-7.0Nb) both show a single-phase (βTi,Nb)$_o$ microstructure after quenching from 1200 °C. When quenched from 1100 °C alloy B16 shows a two-phase microstructure consisting of Ti_3Al and (βTi,Nb)$_o$. The phases were identified by in situ HEXRD measurements.

Table 4 EPMA and HEXRD Results on phase contents, alloy and phase compositions, phase fractions, and lattice parameters of alloys heat-treated at 1200 °C for 30 h (accuracy of the lattice parameters is ± 0.001 Å, n.d.: not determined)

Alloy No	Composition after heat treatment, at.%	Phases	Phase composition measured with EPMA, at.%		Phase fraction, vol.%	Pearson symbol	Lattice parameters, Å	
			Al	Nb			a	c
B5	Ti-24.1Al-25.2Nb	(βTi,Nb)	24.1 ± 0.1	25.2 ± 0.2	100	*cI*2	n.d	
B6	Ti-30.6Al-24.7Nb	(βTi,Nb)$_o$	30.4 ± 0.2	24.5 ± 0.3	97	*cP*2	n.d	
		Nb_2Al	33.4 ± 0.2	36.3 ± 0.5	3	*tP*30	n.d	n.d
B8	Ti-32.3Al-16.9Nb	(βTi,Nb)$_o$	32.3 ± 0.3	16.9 ± 0.3	100	*cP*2	n.d	
B9	Ti-35.2Al-9.8Nb	(βTi,Nb)$_o$	35.2 ± 0.2	9.8 ± 0.2	100	*cP*2	3.219	
B10[b]	Ti-36.5Al-12.8Nb	(βTi,Nb)$_o$	36.5 ± 0.2	12.8 ± 0.2	100	*cP*2	3.220[e]	
B11	Ti-40.0Al-9.5Nb	(αTi)	40.0 ± 0.2	8.3 ± 0.2	16	*hP*2	[d]	
		(βTi,Nb)$_o$	37.4 ± 0.5	10.3 ± 0.1	58	*cP*2	3.218	
		TiAl	45.8 ± 0.2	8.4 ± 0.1	26	*tP*4	4.024	4.064
B12	Ti-39.6Al-19.5Nb	TiAl	45.4 ± 0.2	15.4 ± 0.2	23	*tP*4	n.d	n.d
		(βTi,Nb)	38.1 ± 0.5	19.0 ± 0.3	67	*cP*2	n.d	
		Nb_2Al	36.5 ± 0.3	32.2 ± 0.3	10	*tP*30	n.d	n.d
B13	Ti-43.4Al-4.9Nb[a]	(αTi)	39.9 ± 0.3	5.0 ± 0.2	43	*hP*2	[d]	
		TiAl	45.7 ± 0.3	4.9 ± 0.1	57	*tP*4	n.d	n.d
B14	Ti-43.6Al-5.8Nb	(αTi)	39.7 ± 0.2	6.1 ± 0.2	36	*hP*2	[d]	
		TiAl	45.5 ± 0.4	5.9 ± 0.3	64	*tP*4	n.d	n.d
B15[b]	Ti-41.9Al-12.4Nb	(βTi,Nb)$_o$	37.4 ± 0.3	14.1 ± 0.2	48	*cP*2	3.221	
		TiAl	45.8 ± 0.2	11.6 ± 0.2	52	*tP*4	4.026	4.066
B16	Ti-34.6Al-6.5Nb	(βTi,Nb)$_o$	34.6 ± 0.2	6.5 ± 0.1	100	*cP*2	n.d	
B17	Ti-37.0Al-6.5Nb	(βTi,Nb)$_o$	37.0 ± 0.2	6.5 ± 0.1	100	*cP*2	n.d	

[a]As-cast composition

[b]Alloy contains a small amount of Ti_3Al, which is not considered an equilibrium phase, see Section 3 in Ref. 34

[e]Lattice parameters determined by XRD measurements

[d](αTi) undergoes a phase transformation to Ti_3Al during quenching. Therefore, no lattice parameters could be determined

4 Discussion

Based on the results tabulated above (Tables 2, 3, 4 and 5) and the literature data discussed below, partial isothermal sections of the Ti-rich corner (0 to 60 at.% Al and 0 to 50 at.% Nb) of the Ti-Al-Nb system were determined in the temperature range from 1000 to 1300 °C (Fig. 13–16). For the binary boundary systems Ti-Al and Ti-Nb, the assessed phase diagrams reported in Ref. [8, 25, 39], respectively, were used. The phase fields of (αTi), (βTi,Nb), and Ti_3Al and their temperature-dependent evolution are discussed in more detail below and a reaction scheme for the Ti-Al-Nb system is presented.

4.1 Phase Fields, Solubility Limits, and Ordering Behavior of (βTi,Nb)

4.1.1 The Isolated (βTi,Nb) Phase Field

The isothermal sections at 1000 (Fig. 13) and 1100 °C (Fig. 14) show an isolated (βTi,Nb)$_o$ phase field in the ternary composition space, that has been formed upon heating in a eutectoid reaction from the phases ω_o and TiAl at < 790 °C ((βTi,Nb)$_o$ → TiAl + ω_o).[34] Such an isolated (βTi,Nb)$_o$ phase field has been previously reported by Hellwig et al.[12,13], Li et al.[11], and Eckert et al.[14] at 1000 °C. All authors report the same three tie-triangles

Table 5 EPMA and HEXRD results on phase contents, alloy and phase compositions, phase fractions, and lattice parameters of alloys heat-treated at 1300 °C for 20 h (accuracy of the lattice parameters is ± 0.001 Å, n.d.: not determined)

Alloy No	Composition after heat treatment, at.%	Phases	Phase composition measured with EPMA, at.%		Phase fraction, vol.%	Pearson Symbol	Lattice parameters, Å	
			Al	Nb			a	c
B5	Ti-25.4Al-23.6Nb	(βTi,Nb)	25.4 ± 0.2	23.6 ± 0.3	100	*cI*2	n.d	
B6	Ti-30.7Al-23.9Nb	(βTi,Nb)	30.7 ± 0.2	23.9 ± 0.3	100	*cI*2	n.d	
B8	Ti-32.8Al-16.8Nb	(βTi,Nb)	32.8 ± 0.2	16.8 ± 0.2	100	*cI*2	3.228	
B9	Ti-37.5Al-9.5Nb	(βTi,Nb)	37.5 ± 0.2	9.5 ± 0.1	100	*cI*2	n.d	
B11	Ti-39.5Al-9.7Nb	(βTi,Nb)	39.5 ± 0.2	9.7 ± 0.2	100	*cI*2	3.212	
B12	Ti-39.8Al-19.4Nb	(βTi,Nb)	39.8 ± 0.3	19.4 ± 0.2	100	*cI*2	n.d	
B13	Ti-44.4Al-4.8Nb	(αTi)	44.1 ± 0.2	4.7 ± 0.1	93	*hP*2	[b]	
		TiAl	48.8 ± 0.9	4.7 ± 0.1	7	*tP*4	4.003[a]	4.060[a]
B14	Ti-45.5Al-5.7Nb	(αTi)[b]	44.0 ± 0.2	5.5 ± 0.2	66	*hP*2	[b]	
		TiAl	48.6 ± 0.3	5.4 ± 0.2	34	*tP*4	4.004[a]	4.069[a]
B15	Ti-44.2Al-12.1Nb	(αTi)[b]	43.2 ± 0.6	11.7 ± 0.2	6	*hP*2	[b]	
		(βTi,Nb)	40.8 ± 0.8	13.1 ± 0.2	40	*cI*2	3.217	
		TiAl	46.8 ± 0.6	11.4 ± 0.2	54	*tP*4	4.013	4.074

[a]Lattice parameter determined by XRD measurement

[b](αTi) undergoes a phase transformation to Ti_3Al during quenching. Therefore, no lattice parameters could be determined

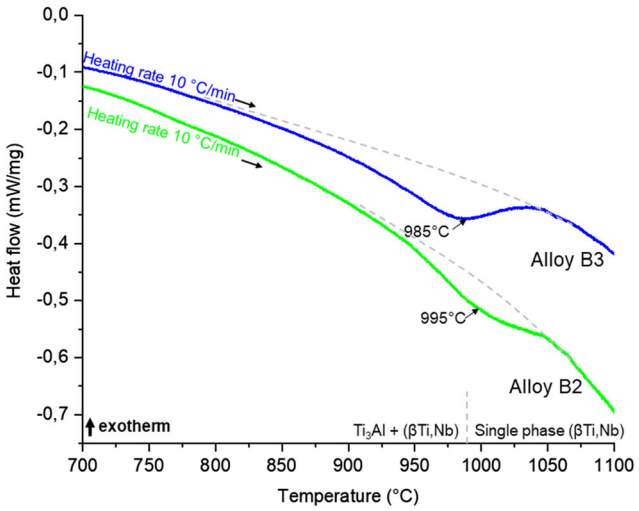

Fig. 6 DTA heating curves of alloys B2 and B3 showing the decomposition of Ti_3Al ending at 985 °C (B3) and 995 °C (B2). The grey dashed lines indicate the baselines

(βTi,Nb)$_o$ + Ti_3Al + TiAl, (βTi,Nb)$_o$ + Ti_3Al + Nb_2Al, and (βTi,Nb)$_o$ + TiAl + Nb_2Al at 1000 °C, which determine the homogeneity range of the isolated (βTi,Nb) phase field. The compositional range in which this (βTi,Nb) phase field is found matches in most cases. The homogeneity range reported here (about 32-35 at. % Al and 11-18 at. % Nb) is like that reported by Hellwig et al.[12,13], while Li et al.[11] report a slightly smaller homogeneity range. The homogeneity range reported by Eckert et al.[14] is shifted to Al contents between 36 and 40 at. % and does not match with the results reported in this study and the previous mentioned results from literature.

According to the present results, the tie-triangle (βTi,Nb)$_o$ + Ti_3Al + TiAl defines the Nb-poor limit of the isolated (βTi,Nb)$_o$ phase field at 1000 °C. It is located at about 36 at. % Al and 11 at. % Nb (alloys B9 and B11, Table 2), which is in good agreement with the studies of Hellwig et al.[13] and Eckert et al.[14], reporting Al contents of about 36 at.% and Nb contents of about 12 at.%. The respective values of Li et al.[11] are shifted to slightly lower Al and higher Nb contents. However, this difference might be explained by some experimental issues in the work of Li et al.[11]. (The authors mention that the weight sums of their EPMA measurements were ranging between 97 and 103 wt.%, which cannot be explained by the (in)accuracy of the EPMA method (being ± 1 wt.% relative[37] but indicates either the presence of additional elements in the sample or problems with the standardization procedure).

From the present results, a maximum Nb content of about 18 at. % is estimated at 1000 °C. This is consistent with the results from Hellwig et al.[13] who reported a Nb content of 17.4 at.% and Al content of 32.5 at.% in the (βTi,Nb)$_o$ phase of the tie-triangle (βTi,Nb)$_o$ + Ti_3Al + Nb_2Al. Additionally, the (βTi,Nb)$_o$ + Ti_3Al tie-line obtained for alloy B8 (Table 2) is located parallel and very

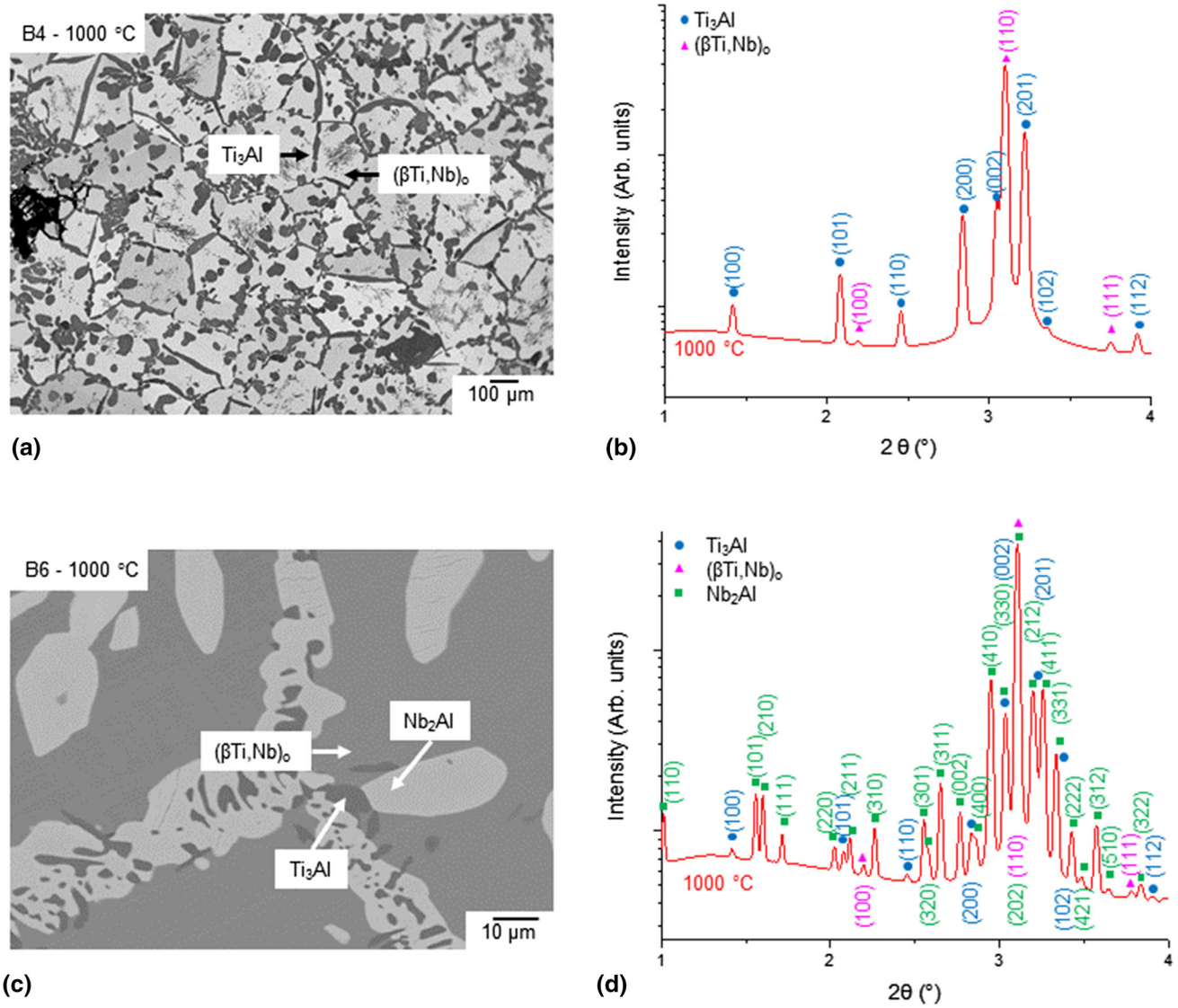

Fig. 7 (a) BSE image of alloy B4 (Ti-24.6Al-14.9Nb) heat-treated at 1000 °C with a two-phase microstructure consisting of (βTi,Nb) (bright) and Ti_3Al (dark); (b) respective HEXRD pattern (with logarithmic intensity scale) confirming the microstructural results; (c) BSE image of alloy B6 (Ti-30.0Al-25.0Nb) heat-treated at 1000 °C showing a three-phase microstructure consisting of Nb_2Al (bright), Ti_3Al (dark) and (βTi,Nb) (grey); (d) respective HEXRD pattern (with logarithmic intensity scale) confirming the microstructural results

close to the $(\beta Ti,Nb)_o + Ti_3Al$ side of the tie-triangle reported by Hellwig et al.[13] Therefore, the position of this tie-triangle is adopted in the present isothermal section at 1000 °C (Fig. 13). The values reported by Li et al.[11] are again shifted compared to the results of Hellwig et al.[13] and those presented here.

At 1100 °C, the phase field of the isolated $(\beta Ti,Nb)_o$ phase is enlarged compared to 1000 °C. In the literature, there are contradicting reports about the presence of this isolated phase field at 1100 °C. In the study by Li et al.[11], the isolated $(\beta Ti,Nb)_o$ phase field is no longer present at 1100 °C. Instead, they report the tie-triangle $Ti_3Al + TiAl + Nb_2Al$ (in an alloy with the composition Ti-39.1Al-17.7Nb) alongside the tie-triangle $(\beta Ti,Nb) + Ti_3Al + Nb_2Al$ (already reported at 1000 °C). The tie-triangle $Ti_3Al + TiAl + Nb_2Al$ must have formed as a result of a ternary peritectoid reaction $(Ti_3Al + TiAl + Nb_2Al \rightarrow (\beta Ti,Nb)_o)$. However, the composition of alloy B12 is located within this tie-triangle. Therefore, a thermal effect should be observed in the DTA measurement because of this invariant reaction. As can be seen from Fig. 17 this is not the case. Additionally, the tie-lines measured for alloy B7 at 1000 and 1100 °C have a similar inclination (Fig. 13 and 14). This suggests that the observed phase equilibria belong to the same phases and no significant change of the Nb contents is observed, which

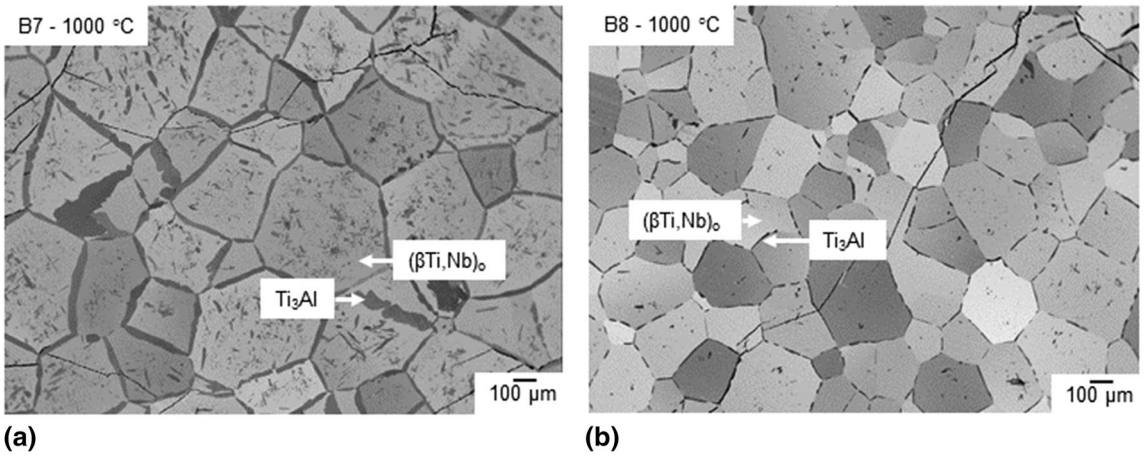

Fig. 8 BSE images of (a) alloy B7 (Ti-32.8Al-12.2Nb) and (b) alloy B8 (Ti-32.4Al-17.3Nb) heat-treated at 1000 °C showing a two-phase microstructure between (βTi,Nb) (bright) and Ti_3Al (dark)

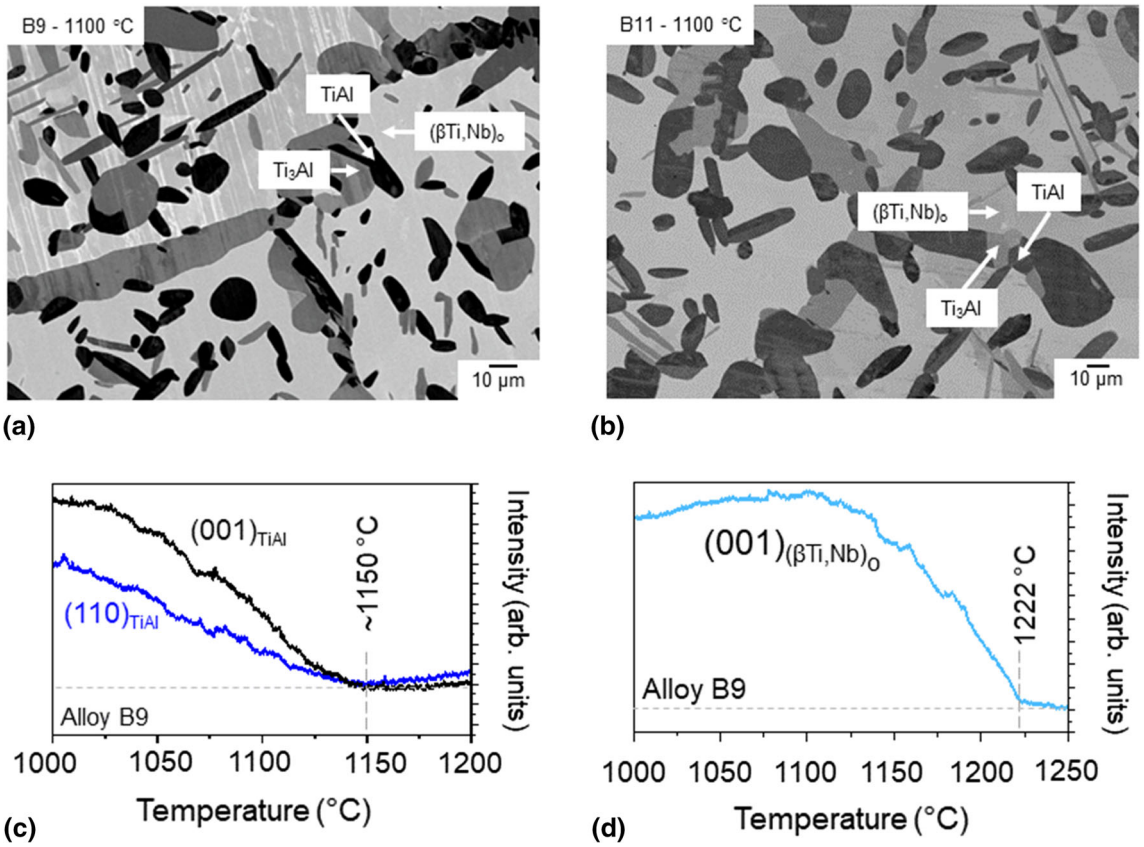

Fig. 9 BSE image of (a) alloy B9 (Ti-37.2Al-10.0Nb) and (b) alloy B11 (Ti-39.6Al-10.0Nb) heat-treated at 1100 °C showing a three-phase microstructure composed of TiAl (dark), Ti_3Al (grey), and $(\beta Ti,Nb)_o$ (matrix); c,d): intensity over temperature plots of (c) the (001) and (110) peak of TiAl, showing the dissolution of TiAl at about 1150 °C in alloy B9 (Ti-37.2Al-10.0Nb), and d) the (001) superstructure reflection of $(\beta Ti,Nb)_o$ showing the disordering of $(\beta Ti,Nb)_o$ at 1222 °C (data obtained by in situ HEXRD measurements)

would be the case if the isolated $(\beta Ti,Nb)_o$ phase field and the $(\beta Ti,Nb)$ solid solution merge into one phase field, as it is observed at 1200 °C (Fig. 15). Furthermore, experimental results of Bendersky et al.[40,41] for two alloys (Ti-37.5Al-20Nb and Ti-37.5Al-12.5Nb) heat-treated at 1100 °C show the presence of two tie-triangles ($(\beta Ti,Nb)_o + Ti_3Al + TiAl$ and $(\beta Ti,Nb)_o + TiAl + Nb_2Al$), which agree with the here presented results and

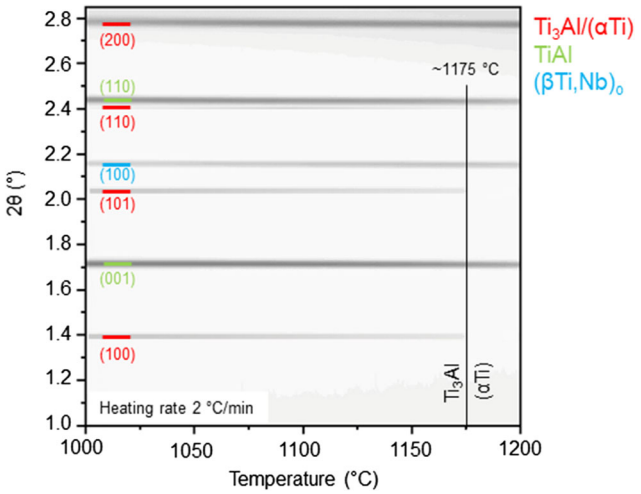

Fig. 10 Plot of the in situ HEXRD measurement (heating rate 2 °C/min) of alloy B11 (Ti-39.6Al-10.0Nb) in the Temperature range between 1000 and 1200 °C showing the presence of TiAl + Ti_3Al + $(\beta Ti,Nb)_o$ above 1000 °C. The (100) and (101) superstructure reflections of Ti_3Al are observed up to ~ 1175 °C. At higher temperatures (αTi) is stable instead

contradict those from Li et al.[11] . From the results presented, it is concluded that at 1100 °C $(\beta Ti,Nb)_o$ still exists as an isolated phase field. This conclusion also agrees with the results from Eckert et al.[14].

4.1.2 The (βTi,Nb) Solid Solution

In addition to the isolated $(\beta Ti,Nb)_o$ phase field, there exists a large phase field of the disordered (βTi,Nb) solid solution in the isothermal sections at 1000 (Fig. 13) and 1100 °C (Fig. 14), which extends starting from the binary Ti-Nb system far into the ternary composition triangle. Above a certain Al content (roughly about 20 at. % at 1000 °C and 25 at. % at 1100 °C), the bcc-type solid solution becomes *B*2-ordered. The maximum Al solubility of the (βTi,Nb) solid solution at 1000 and 1100 °C corresponds to the composition of the ordered $(\beta Ti,Nb)_o$ phase in the three-phase equilibrium with Ti_3Al and Nb_2Al (see Fig. 13 and 14). At 1000 °C, alloy B6 lies in this tie-triangle and a solubility of 29.1 at. % Al is obtained for the $(\beta Ti,Nb)_o$ phase (Table 2). This value increases only slightly at 1100 °C (Fig. 13). The maximum values for the Al solubility reported in the literature vary between 20-30 at. %, and the corresponding values for Nb are in the same range.[11,13]

At 1200 and 1300 °C (Fig. 15 and 16), only one $(\beta Ti,Nb)/(\beta Ti,Nb)_o$ phase field is observed, which is the consequence of a reaction between the two tie-triangles Ti_3Al + Nb_2Al + $(\beta Ti,Nb)_o$ at an unknown temperature between 1100 and 1200 °C. The calculations of Witusiewicz et al.[24] predict a eutectoid reaction $(\beta Ti,Nb)_o \rightarrow Nb_2Al + Ti_3Al$ with a reaction temperature of 1073 °C. However, as shown in the preceding section 4.1.1, this temperature must lie above 1100 °C. Since the two tie-triangles $(\beta Ti,Nb)_o$ + Ti_3Al + Nb_2Al are very close to each other at 1100 °C (Fig. 14), the reaction temperature is estimated here as 1110 ± 10 °C.

The solubility of Al in (βTi,Nb) reaches more than 40 at.% Al (alloy B15) at 1300 °C (Fig. 16 and Table 5), which is in agreement with the values reported in the literature.[9,15,27] The stability range of the *B*2-ordered (βTi,Nb) phase was investigated by DTA in our preceding study Ref. 38, and the respective composition ranges are marked by dotted lines in the isothermal sections in Fig. 13-15. With increasing temperature, the compositional range of the *B*2-ordered (βTi,Nb) phase narrows, and at 1200 °C the $(\beta Ti,Nb)_o$ phase field separates the disordered (βTi,Nb) phase into two fields (Fig. 15). The ordered $(\beta Ti,Nb)_o$ phase is stable up to a maximum temperature of about 1250 °C, which is reached at a composition on the line $Ti_2(Al,Nb)$ as described in Ref. 38.

4.2 Phase Fields of (αTi) and Ti_3Al

4.2.1 The Ti_3Al phase Field

At 1000 °C, Ti_3Al is stable in a composition range of Ti-(23-37) Al-(0-15)Nb with the maximum Nb content reached in the three-phase equilibrium with (βTi,Nb) and Nb_2Al (Fig. 13). This agrees with the results shown in Refs. 11, 13, where the same solubility value of 15 at. % Nb was reported. At 1100 °C, the maximum Nb content in Ti_3Al remains the same, but considered as a function of Al content, the Nb solubility shows a very particular behaviour. As is well visible in the isothermal section in Fig. 14, there is a local solubility minimum of only 5.5 at. % Nb located at 35.0 at. % Al, which is related to the growing $(\beta Ti,Nb)_o$ phase field. The respective two-phase equilibrium $(\beta Ti,Nb)_o$ + Ti_3Al is observed in alloy B16 (see Table 3 and Fig. 18). At higher Al contents, the Nb solubility increases again up to ~ 8 at. % (reached in the three-phase equilibrium $(\beta Ti,Nb)_o$ + Ti_3Al + TiAl that occurs in alloys B9 and B11 (Table 3 and Fig. 9a,b). In the isothermal section at 1100 °C presented by Li et al.[11], the Ti_3Al phase field has a qualitatively very similar shape with a local minimum of the Nb content at intermediate Al contents. However, this minimum appears to be less pronounced than indicated in the present results, which is related to the absence of the isolated $(\beta Ti,Nb)_o$ phase field in the isothermal section shown by Li et al.[11].

In the isothermal sections at 1200 and 1300 °C (Fig. 15 and 16), Ti_3Al is no longer present (except for a single point at the Ti-Al binary boundary at 1200 °C) as also reported by Kainuma et al.[15]. However, there are two

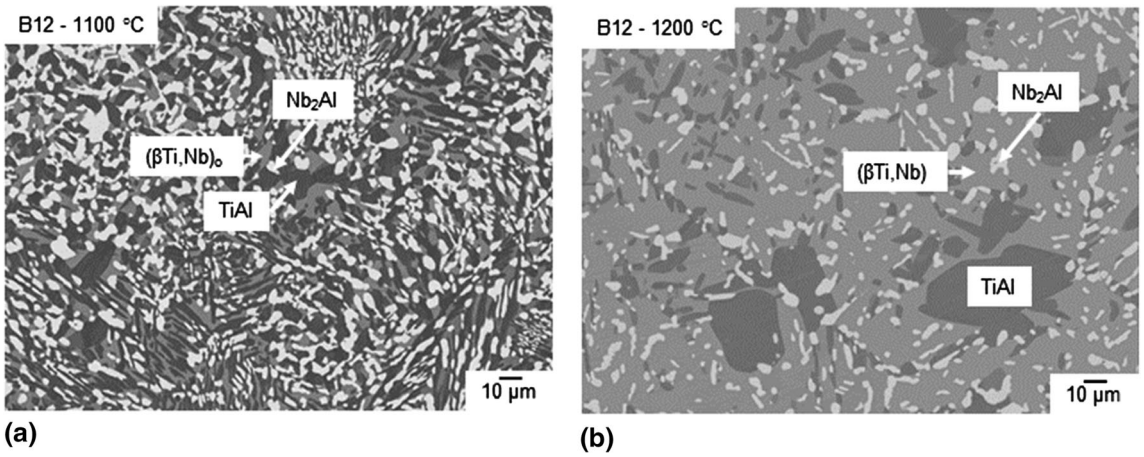

Fig. 11 BSE image of alloy B12 (Ti-39.8Al-19.9Nb) heat-treated at (a) 1100 °C showing a three-phase microstructure between TiAl (dark), Nb_2Al (bright) and (βTi,Nb) (grey), and (b) 1200 °C showing the same three phases but with the (βTi,Nb) phase being disordered now according to the DTA results

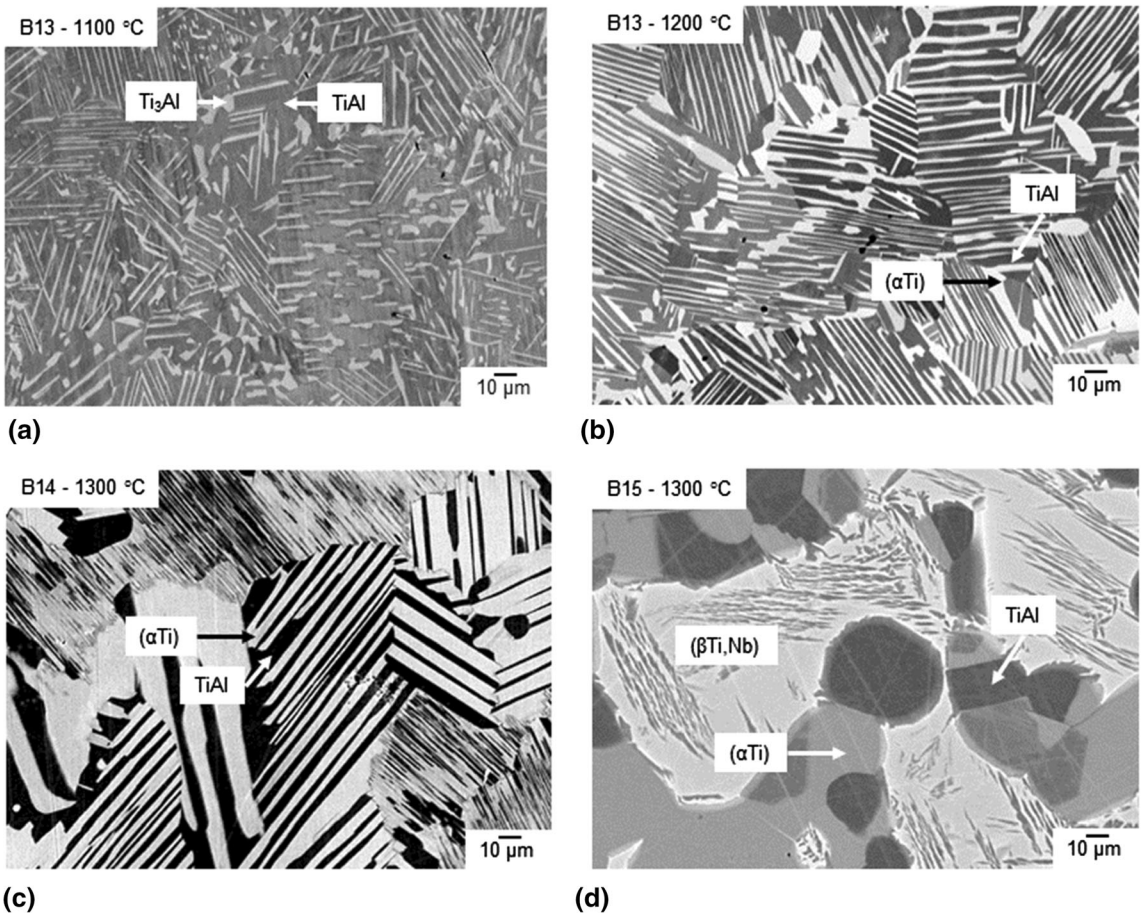

Fig. 12 BSE image of (a) alloy B13 (Ti-43.4Al-4.9Nb) heat-treated at 1100 °C showing a two-phase microstructure consisting of TiAl (dark) and Ti_3Al (bright); (b) alloy B13 heat-treated at 1200 °C showing a two-phase microstructure consisting of TiAl (dark) and (αTi) (bright); (c) alloy B14 (Ti-45.8Al-5.9Nb) heat-treated at 1300 °C showing a two-phase microstructure consisting of TiAl (dark) and (αTi) (bright); d) alloy B15 (Ti-44.7Al-12.3Nb) heat-treated at 1300 °C showing the three-phase equilibrium between TiAl (dark), (αTi) (grey) and (βTi,Nb) (bright)

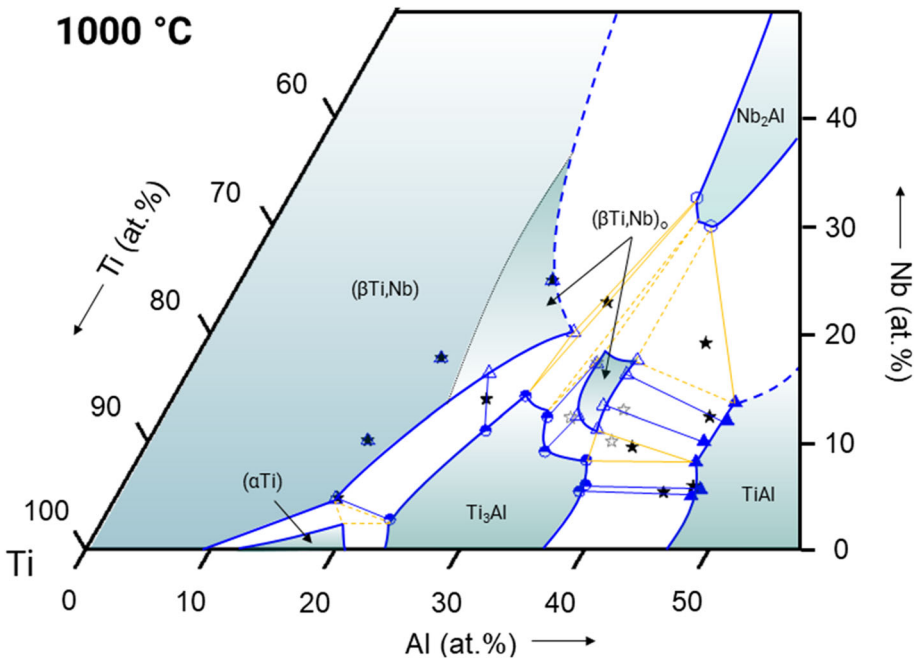

Fig. 13 Partial isothermal section at 1000 °C based on the experimental results tabulated in Table 2. The measured overall compositions of the heat-treated samples are indicated by black stars, grey stars represent nominal or as-cast composition, the yellow lines mark the three-phase equilibria, and blue symbols and lines mark the results from bulk alloys and the resulting phase boundaries

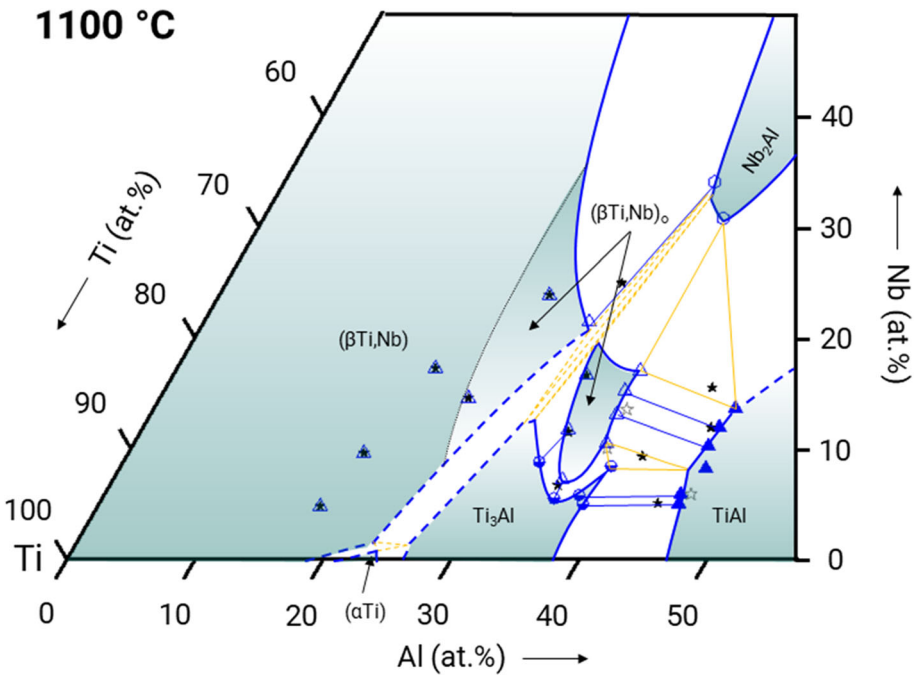

Fig. 14 Partial isothermal section at 1100 °C based on the experimental results tabulated in Table 3 (symbols see Fig. 13)

other studies that propose a stable Ti_3Al phase field at 1200 °C extending into the ternary composition space.[26,42] Based on the accepted decomposition of Ti_3Al at 1200 °C in the binary Ti-Al system[8,25] this phase field must be connected to the binary system at a single point (composition of Ti_3Al in the binary). In order to study the possible existence of a Ti_3Al phase field in the ternary system at 1200 °C in more detail, the two alloys B16 and B17 were synthesized. Both alloys were found to be single-phase after quenching from 1200 °C (with compositions of Ti-34.6Al-6.5Nb and Ti-37.0Al-6.5Nb), and from in situ HEXRD measurements of alloy B16 it is concluded that this alloy is single-phase (βTi,Nb)$_o$ at 1200 °C. This is evident from the intensity of the (200) and (201) peaks of Ti_3Al, which vanish at an extrapolated temperature of about 1175 ± 10 °C (Fig. 18b). However, this does not completely rule out the existence of a Ti_3Al phase field at 1200 °C, since it is still possible that this phase field is stable at Nb contents below 6 at. % and therefore was not found in the alloys studied here. Unfortunately, there is no

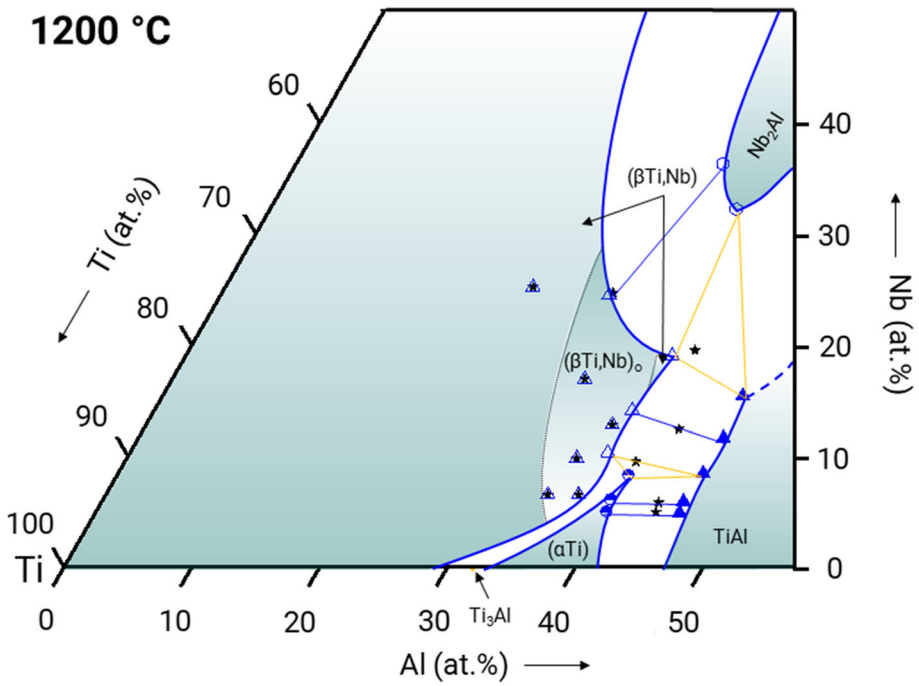

Fig. 15 Partial isothermal section at 1200 °C based on the experimental results tabulated in Table 4 (symbols see Fig. 13)

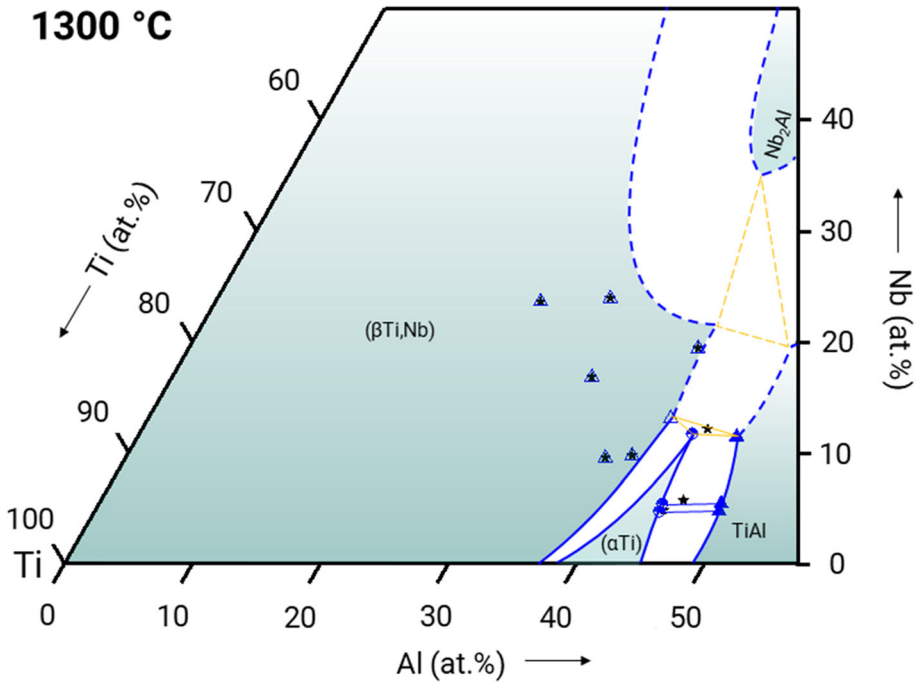

Fig. 16 Partial isothermal section at 1300 °C based on the experimental results tabulated in Table 5 (symbols see Fig. 13)

data available in literature that would give indications about the existence of Ti_3Al at 1200 °C at this low Nb levels. In Fig. 19, the just described possibility of the existence of Ti_3Al at 1200 °C is superimposed on the isothermal section from Fig. 15 with black dashed lines. If such a phase field exists at 1200 °C, and since this is the decomposition temperature in the binary system, a Ti_3Al island in the ternary composition space must exist at temperatures just above 1200 °C, i.e., the maximum stability of Ti_3Al would be reached in the ternary system near, but not at, the binary boundary. Although this possibility cannot be ruled out, it should be considered less likely, and we assume that the isothermal section presented in Fig. 15 is more realistic.

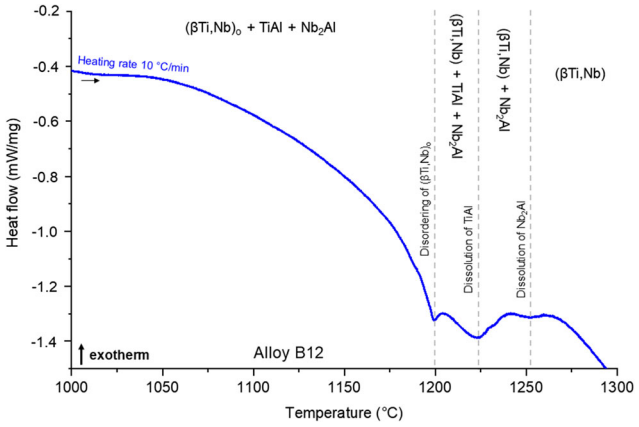

Fig. 17 DTA heat flow measurement of alloy B12 (Ti-39.8Al-19.9Nb) showing no peak between 1000 and 1100 °C, which indicates that no invariant reaction takes place in this temperature interval. At higher temperatures, the disordering of $(\beta Ti,Nb)_o$ at 1199 °C and the dissolution of TiAl at 1224 °C and Nb_2Al at 1253 °C are visible

4.2.2 The (αTi) Solid Solution

In the binary Ti-Al system, the (αTi) solid solution has two separated single-phase fields (at low temperatures and low Al contents, and at high temperatures and intermediate Al contents).[8,25] which also affects the ternary Ti-Al-Nb system.

The Ti-rich (αTi) solid solution is stable up to 1170 °C in the binary Ti-Al system and decomposes at this temperature by a peritectoid reaction into (*β*Ti,Nb) + Ti_3Al.[8,25] If the same shrinking of the phase field also occurs in the ternary system, the Nb solubility in (αTi) must decrease with increasing temperature compared to the value of 3.7 at. % measured at 900 °C for alloy B1.[34] This assumption is supported by the observation that alloy B1 at 1000 °C no longer contains the (αTi) phase, which is more and more displaced by the growing (*β*Ti,Nb) phase field as the temperature increases. For the isothermal sections at 1000 and 1100 °C in Fig. 4 and 13, tentative values of 2 and 1 at. %, respectively, were estimated for the solubility of Nb in the shrinking phase field of (αTi).

The Al-rich (αTi) solid solution forms at 1120 °C in a eutectoid reaction from Ti_3Al and TiAl in the binary Ti-Al system.[8,25] It is observed at 1200 °C in the ternary alloys B11, B13, and B14 (Fig. 15). The solubility of Nb is 8.3 at. % at 1200 °C and increases to 11.7 at. % at 1300 °C (Fig. 3 and Tables 4 and 5). The values reported in the literature differ between 11 and 16 at. % Nb, while the associated Al content always agrees (about 43-44 at. %).[9,15,27] A possible reason for the differences in Nb content could be the oxygen content, as discussed in Ref. 43 The eutectoid formation temperature increases with increasing Nb content of the three alloys B13, B14, and B11 (1143 °C, 1159 °C, and 1171 °C, respectively; see Ref. 38 where the corresponding alloy designations are A1, A2, and A3). This increase in temperature is also consistent with other experimental results from the literature on alloys with different compositions.[24,44-47]

4.3 Invariant Reactions and Reaction Scheme

The reaction scheme (sometimes called "Scheil scheme" after his inventor Erich Scheil[48]) of the Ti-Al-Nb system is presented in Fig. 20, and a list of all invariant reactions is given in Table 7. Since in the current work no reactions with the liquid phase (L) were studied, the respective information was adopted from the scheme presented by Witusiewicz et al.[24] The binary phase $Ti_{2+x}Al_{5-x}$ is not considered as an equilibrium phase in the assessed Ti-Al phase diagram[8,25] and, therefore, the transition reaction ($L + TiAl \rightarrow TiAl_3 + Ti_{2+x}Al_{5-x}$) shown in the reaction scheme of Witusiewicz et al.[24] is excluded here. Types and temperatures of reactions which take place in the temperature range from 700 to 1300 °C are based on the experimental results discussed here and in our preceding publications.[34,38] The reaction temperatures in the binary systems are taken from the recent assessments of these systems.[8,25,39,49] For consistency, the phase designation "(*β*Ti,Nb)" is also used in the binary systems. All phases that occur in the ternary system and are not listed in Table 1 in Ref. 34 are summarized with some crystallographic information in Table 6. The two binary phases $TiAl_3$ and $NbAl_3$ have the same tetragonal crystal structure and share a common phase field that connects both binary systems along a constant Al content of 75 at.%. Therefore, this phase is designated as $(Ti,Nb)Al_3$ in the ternary system.

4.3.1 B2-Ordering of (βTi,Nb)

Witusiewicz et al.[24] assume that *B*2-ordering of (*β*Ti,Nb) occurs already in the binary Ti-Al system. However, since there is no experimental evidence for this[25] it is assumed here that the *B*2-ordered $(\beta Ti,Nb)_o$ phase field is restricted to the ternary composition space with a composition range as described in section 4.1 and shown in the isothermal sections in Fig. 13-15. Therefore, three reactions (ec_1 to ec_3, see Table 7) are necessary where the ordered phase field contacts with the respective phase boundary of a two-phase field. The eutectoid character of these reactions is a result of the growth of the (*β*Ti,Nb) phase field in each direction with increasing temperature. The temperatures of these reactions are estimated based on the disordering temperatures determined in Ref. 38 and the isothermal sections presented here. At 1200 °C (Fig. 15), the (*β*Ti,Nb) solid solution is separated into two separated fields by a

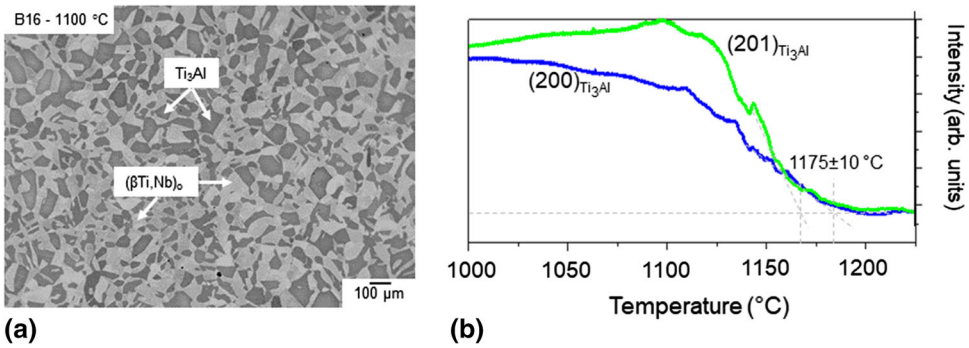

Fig. 18 (a) BSE image of alloy B16 (Ti-35.0Al-5.0Nb) heat-treated at 1100 °C showing a two-phase microstructure between $(\beta Ti,Nb)_o$ (bright) and Ti_3Al (dark), (b) intensity of the (200) and (201) HEXRD peaks of Ti_3Al showing that Ti_3Al is no longer present above 1175 ± 10 °C in alloy B16

Table 6 Crystallographic information for the phases which are not already listed in Table 1 of Ref. (34)

Phase	Crystal system	Pearson symbol	Space group	Strukturbericht designation	Reference
$TiAl_2$	tetragonal	*tI*24	$I4_1/amd$	…	[50]
$TiAl_3/NbAl_3$ $(Ti,Nb)Al_3$	tetragonal	*tI*4	*I*4/*mmm*	$D0_{22}$	[51]

Table 7 List of invariant reactions in the ternary Ti-Al-Nb system with corresponding reaction type (E,e = ternary (E) or pseudo-binary (e) eutectic/eutectoid reaction; P, p = ternary (P) or pseudo-binary (p) peritectic/peritectoid reaction; U = transition type reaction; the addition of "c" to a reaction underlines the "chemical ordering" taking place in these reactions (order/disorder of $(\beta Ti,Nb)$) and is adopted from Witusiewicz et al.[52]

Reaction	Type	Temperature, °C	Ref
$L + Nb_3Al \rightarrow Nb_2Al + (\beta Ti,Nb)$	U_1	1930	[24]
$L + Nb_2Al + (\beta Ti,Nb) \rightarrow TiAl$	P_1	1739	[24]
$L \rightarrow (Ti,Nb)Al_3 + TiAl$	e_1	1585	[24]
$L \rightarrow Nb_2Al + (Ti,Nb)Al_3 + TiAl$	E_1	1558	[24]
$L + (\beta Ti,Nb) + TiAl \rightarrow (\alpha Ti)$	P_2	1518	[24]
$(\beta Ti,Nb) \rightarrow Nb_2Al + (\beta Ti,Nb)_o$	ec_1	1245 ± 2	[38], This work
$(\beta Ti,Nb) \rightarrow (\alpha Ti) + (\beta Ti,Nb)_o$	ec_2	1230 ± 5	[38], This work
$(\beta Ti,Nb) \rightarrow (\beta Ti,Nb)_o + TiAl$	ec_3	1220 ± 5	[38], This work
$(\beta Ti,Nb) + TiAl \rightarrow (\alpha Ti) + (\beta Ti,Nb)_o$	Uc_1	1201	[38], This work
$(\beta Ti,Nb) \rightarrow Nb_2Al + (\beta Ti,Nb)_o + TiAl$	Ec_1	1199	[38], This work
$(\beta Ti,Nb) \rightarrow (\alpha Ti) + (\beta Ti,Nb)_o + Ti_3Al$	Ec_2	1190 ± 10	[38], This work
$(\alpha Ti) + (\beta Ti,Nb)_o \rightarrow Ti_3Al + TiAl$	U_2	1175 ± 10	This work
$(\beta Ti,Nb)_o \rightarrow Nb_2Al + Ti_3Al$	e_4	1110 ± 10	This work
$Nb_2Al + (\beta Ti,Nb)_o + Ti_3Al \rightarrow O$	P_3	970 ± 5	[38], This work
$Nb_2Al + (\beta Ti,Nb)_o \rightarrow (\beta Ti,Nb) + O$	Uc_2	955 ± 15	This work
$Nb_2Al + (\beta Ti,Nb) \rightarrow Nb_3Al + O$	U_3	930 ± 10	This work
$Nb_2Al + (\beta Ti,Nb)_o + TiAl \rightarrow \omega_o$	P_4	920 ± 10	[38], This work
$(\beta Ti,Nb)_o + Ti_3Al + TiAl \rightarrow \omega_o$	P_5	920 ± 10	[38], This work
$Nb_2Al + Ti_3Al \rightarrow (\beta Ti,Nb)_o + O$	U_4	898 ± 1	[34]
$Nb_2Al + (\beta Ti,Nb)_o \rightarrow O + \omega_o$	U_5	897	[34]
$(\beta Ti,Nb)_o + Ti_3Al \rightarrow O + \omega_o$	U_6	897	[34]
$(\beta Ti,Nb)_o \rightarrow (\beta Ti,Nb) + Ti_3Al + O$	Ec_3	880 ± 10	[34]
$(\beta Ti,Nb)_o \rightarrow O + \omega_o$	e_6	850 ± 45	[34]
$(\beta Ti,Nb)_o \rightarrow TiAl + \omega_o$	e_7	$< 790^c$	[34]

*B*2-ordered $(\beta Ti,Nb)_o$ phase field. Therefore, the three reactions (ec_1 to ec_3) must take place above 1200 °C. The disordering temperature of $(\beta Ti,Nb)$ in alloy B6 (alloy A10 in Ref. 38) is 1243 °C. Based on this temperature and the fact that the maximum disordering temperature is 1248 °C[38] in an alloy with slightly higher Al content, it is estimated that the reaction $(\beta Ti,Nb) \rightarrow Nb_2Al + (\beta Ti,Nb)_o$ (ec_1) takes place at 1245 ± 2 °C. From

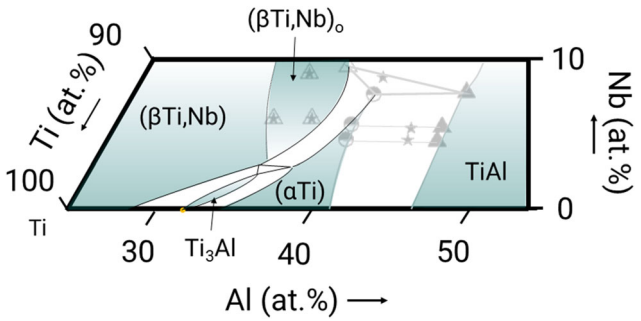

Fig. 19 Possible Ti_3Al phase field at 1200 °C (black) superimposed on an enlarged part (25-55 at.% Al and 0-10 at.% Nb) of the isothermal section (grey) from Fig. 15

the disordering temperature (1237 °C) measured for alloy B7 (alloy A5 in Ref. 38), the temperature of reaction ec_2 is estimated to be 1230 ± 5 °C. The approximate value of the reaction temperature of (βTi,Nb) → (βTi,Nb)$_o$ + TiAl (ec_3) is based on the disordering temperature of alloy B10 (alloy A6 in Ref. 38) and is 1220 ± 5 °C. As a result of reaction ec_3, two (βTi,Nb)/(βTi,Nb)$_o$ second-order transition points exist on the phase boundary between the (βTi,Nb) solid solution and the two-phase field (βTi,Nb) + TiAl. With decreasing temperature the Nb-lean (βTi,Nb)/(βTi,Nb)$_o$ transition point shifts towards the tie-triangle (βTi,Nb) + TiAl + (αTi). This tie-triangle is observed in alloy B11 at 1200 °C (Table 4) and the disordering temperature of (βTi,Nb)$_o$ is measured to be 1201 °C (alloy A3 in Ref. 38). This temperature represents the reaction temperature of the transition-type reaction (βTi,Nb) + TiAl → (αTi) + (βTi,Nb)$_o$ (Uc_1). The Nb-rich (βTi,Nb)/(βTi,Nb)$_o$ + TiAl line "shifts" towards the tie-triangle (βTi,Nb) + TiAl + Nb_2Al observed in alloy B12. The disordering temperature in this alloy is 1199 °C (alloy A12 in Ref. 38), which corresponds the reaction temperature of the eutectoid type reaction (βTi,Nb) → Nb_2Al + (βTi,Nb)$_o$ + TiAl (Ec_1). The invariant reaction Ec_2 is assumed to take place between reactions Ec_1 and U_2 because otherwise very complex reactions including Ti_3Al and (βTi,Nb)$_o$ would be necessary. The reaction temperature 880 ± 10 °C for reaction Ec_3 ((βTi,Nb)$_o$ → (βTi,Nb) + Ti_3Al + O) is based on in situ HEXRD measurements of alloy B4, which show that above 880 °C the (100) superstructure reflex of (βTi,Nb)$_o$ phase occurs for the first time.

4.3.2 Reactions Involving (αTi) and Ti_3Al

Witusiewicz et al.[24] conclude from their experimental results that there should be a shallow temperature maximum on the eutectoid line involving (αTi) + Ti_3Al + TiAl. The composition of this maximum is not given but results in a ternary eutectoid reaction (αTi) → Ti_3Al + (βTi,Nb)$_o$ + TiAl (cf. reaction Ed1 in Fig. 11 of Ref. 24) at 1164 °C. However, based on our experimental results we assume a reaction sequence with a transition-type reaction instead of the eutectoid reaction proposed by Witusiewicz et al.[24] This also excludes the shallow temperature maximum.

As a result of the eutectoid reaction (αTi) → Ti_3Al + TiAl at 1120 °C, the tie-triangle (αTi) + Ti_3Al + TiAl must be present at higher temperatures. At 1200 °C, the tie-triangle (αTi) + (βTi,Nb)$_o$ + TiAl is observed instead (Fig. 15). This tie-triangle is assumed to have formed as a result of the transition reaction (αTi) + (βTi,Nb)$_o$ → Ti_3Al + TiAl involving the just mentioned tie-triangle (αTi) + Ti_3Al + TiAl and the tie-triangle Ti_3Al + (βTi,Nb)$_o$ + TiAl found at 1100 °C in alloys B9 and B11 (Table 3). This reaction is estimated to take place at 1175 ± 10 °C, corresponding to the transformation temperature determined by in situ HEXRD in alloy B11 (Fig. 10). This type of reaction was already proposed by Takeyama et al.[42] and was observed between 1140 and 1200 °C in the chemically related system Ti-Al-V (V and Nb both are group 5 transition metals) by Shaaban et al.[53] As a result of the transition-type reaction, a second tie-triangle (αTi) + Ti_3Al + (βTi,Nb)$_o$ exists above the transformation temperature. However, since Ti_3Al is assumed to decompose at 1200 °C (see section 4.2.1), this three-phase equilibrium is not observed in the present experiments.

4.3.3 Reactions Involving Ternary Intermetallic Phases

Most of the reactions involving the two intermetallic compounds ω_o (hexagonal, *hP*6, $P6_3/mmc$) and O (orthorhombic, *oC*16, *Cmcm*) in the Ti-Al-Nb system were already discussed in Part I (Ref. 34) dealing with the phase equilibria between 700 and 900 °C and/or in our preceding article Ref. 38 about the kinetics of the reactions involving these two phases. Therefore, here we only add some brief information about the estimation of the remaining reaction temperatures of the invariant reactions.

From the experimental results discussed in Ref. 34 it is concluded that two separate phase fields of the ω_o phase exist at 900 °C (cf. Figure 15 in Ref. 34). The dissolution temperatures of the Nb-lean and Nb-rich ω_o phase field are based on the temperatures determined in Ref. 38 for alloys B7 (alloy A5 in Ref. 38) and B12 (alloy A9 in Ref. 38), respectively. Two peritectoid reactions P_4/P_5 facilitate this dissolution at around 920 ± 10 °C (Table 7). In a similar type of reaction (Nb_2Al + (βTi,Nb)$_o$ + Ti_3Al → O, P_3) the O phase decomposes. The reaction temperature is estimated to be 970 ± 5 °C which is slightly above the highest temperature measured (963 °C in alloy A10 in Ref. 38) for the dissolution of the O phase. For this reaction to

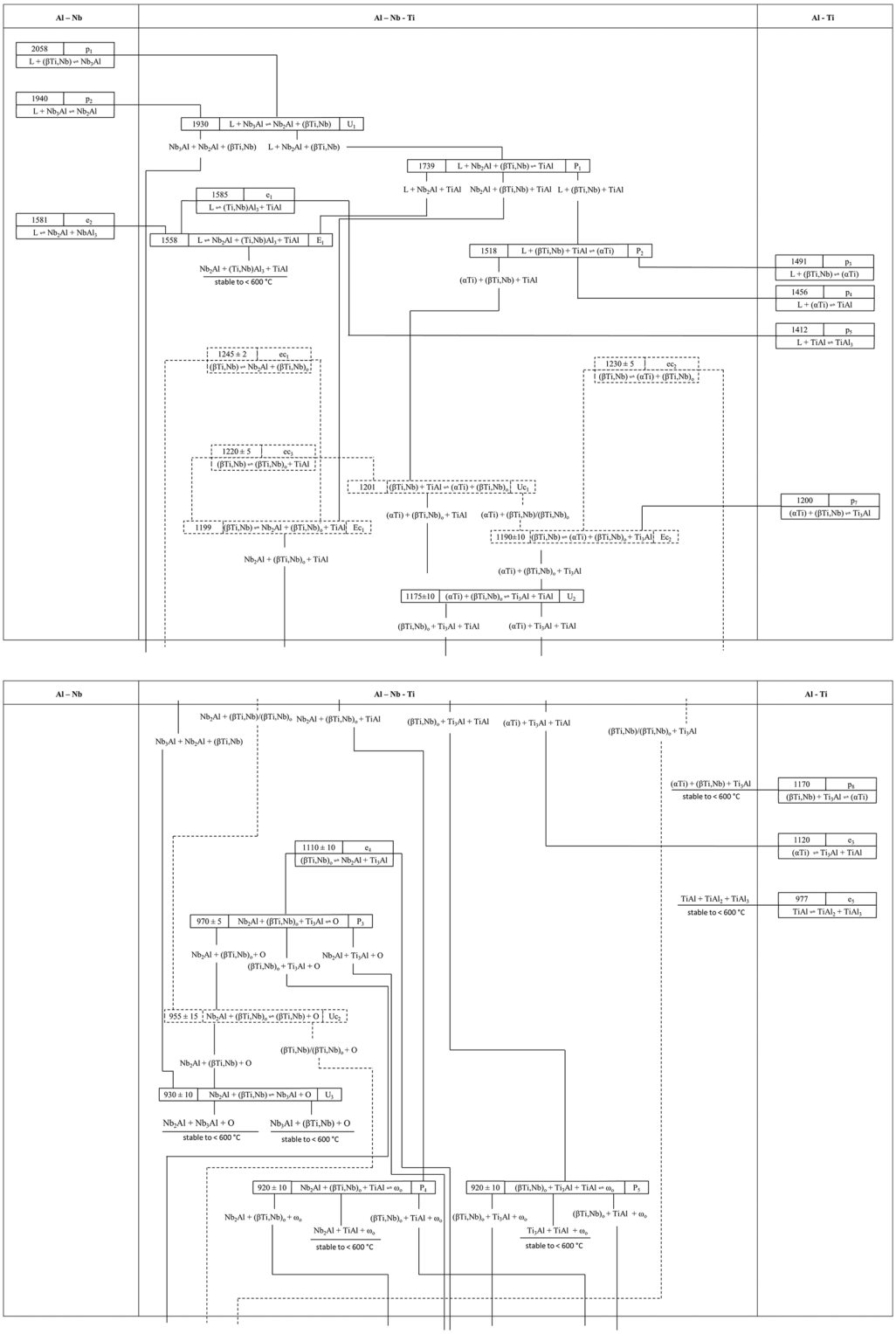

Fig. 20 Reaction scheme of the Ti-Al-Nb system from the liquid phase down to 600 °C. Reactions including the liquid phase are based on Witusiewicz et al.[24] The other reactions are based on the here presented results and the results discussed in Ref. 34, 38. Dashed lines mark reactions related to ordering/disordering of the (βTi,Nb) phase (it should be noted that due the second-order nature of these reactions, the dashed lines do not correspond to new three-phase tie-triangles but instead represent new two-phase equilibria. This is described in detail by Witusiewicz et al.[52]

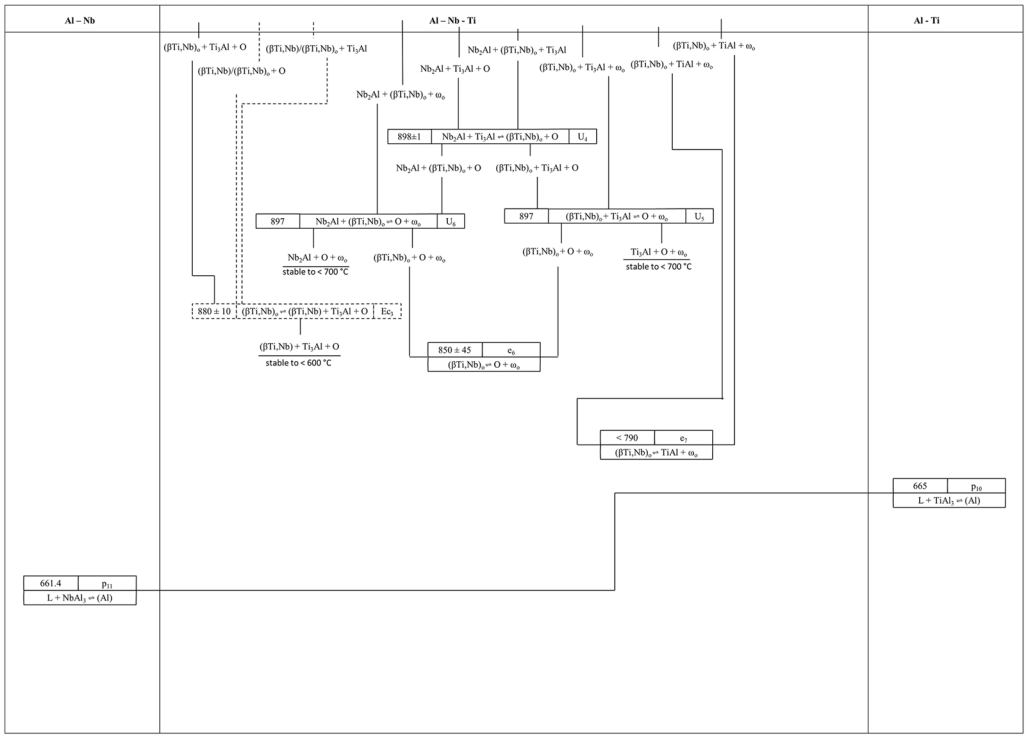

Fig. 20 continued

take place the two tie-triangles (βTi,Nb) + Nb_3Al + O and Nb_3Al + Nb_2Al + O present at 900 °C (cf. Figure 15 in Ref. 34) need to undergo a transition type reaction (U_3) which is estimated to take place at 930 ± 10 °C since they are already very close together at 900 °C. For this reaction Witusiewicz et al.[24] calculated a reaction temperature of 971 °C, however, they did not consider the ordering of the (βTi,Nb) phase, which is necessary for reaction P_3 to take place. Furthermore, the transition temperatures determined for the O to (βTi,Nb) transition in Ref. 38 are all below 970 °C which means that the ordering needs to take place between reactions U_3 and P_3. Therefore, the reaction temperature of Uc_2 is estimated to be 955 ± 15 °C.

5 Conclusions

Partial isothermal sections of the Ti-rich corner of the Ti-Al-Nb system at 1000, 1100, 1200, and 1300 °C, covering the composition range (0-60) at.% Al and (0-50) at.% Nb, were determined based on experimental investigations of a series of heat-treated alloys by EPMA, (in situ HE)XRD, and DTA.

The results confirm that an isolated (βTi,Nb)$_o$ phase field coexists with a (βTi,Nb) solid solution at 1000 and 1100 °C. The isolated (βTi,Nb)$_o$ phase field extends parallel to the Ti-Nb axis between 11 and 18 at.% Nb at 1000 °C and 6.5 and 20 at.% Nb at 1100 °C, with Al contents between 32 and 36 at.%. It merges with the phase field of the (βTi,Nb)/(βTi,Nb)$_o$ solid solution phase above 1100 °C because of a eutectoid reaction (βTi,Nb)$_o$ → Nb_2Al + Ti_3Al. The maximum solubility of Al in (βTi,Nb) increases up to 40 at.% at 1300 °C.

The Nb solubility in Ti_3Al is maximum at 1000 and 1100 °C reaching a value of about 15 at.%. The above mentioned fast growing homogeneity range of the (βTi,Nb)$_o$ phase also affects the phase field of Ti_3Al and leads to a local minimum of the Nb content (6.5 at.%) around 35 at.% Al at 1100 °C. At temperatures above 1100 °C, the Nb solubility rapidly decreases and Ti_3Al is no longer stable above 1200 °C. The Al-rich (αTi) phase forms from the binary Ti-Al system at 1120 °C and its phase field grows further into the ternary composition triangle with increasing temperature.

Finally, a reaction scheme for the Ti-Al-Nb system has been prepared, which is intended to be an improvement of the earlier version presented by Witusiewicz et al.[24] and is based on our combined results on phase transformations and phase equilibria between 700 and 1300 °C reported in Ref. 38, in Part I.[34] and in the present investigations.

Acknowledgments The authors gratefully acknowledge funding from the Clean Sky 2 Joint Undertaking under the European Union's Horizon 2020 research and innovation program under grant agreement No. 820647.

Funding Open Access funding enabled and organized by Projekt DEAL.

References

1. B.P. Bewlay, S. Nag, A. Suzuki, and M.J. Weimer, TiAl Alloys in Commercial Aircraft Engines, *Mater. High Temp.*, 2016, **33**(4–5), p 549–559. https://doi.org/10.1080/09603409.2016.1183068
2. X. Wu, Review of Alloy and Process Development of TiAl Alloys, *Intermetallics*, 2006, **14**, p 1114–1122. https://doi.org/10.1016/j.intermet.2005.10.019
3. T. Tetsui, K. Shindo, S. Kaji, S. Kobayashi, and M. Takeyama, Fabrication of TiAl Components by Means of Hot Forging and Machining, *Intermetallics*, 2005, **13**(9), p 971–978. https://doi.org/10.1016/j.intermet.2004.12.012
4. H. Clemens, W. Wallgram, S. Kremmer, V. Güther, A. Otto, and A. Bartels, Design of Novel β-Solidifying TiAl Alloys with Adjustable β/B2-Phase Fraction and Excellent Hot-Workability, *Adv. Eng. Mater.*, 2008, **10**(8), p 707–713. https://doi.org/10.1002/adem.200800164
5. B.P. Bewlay, M. Weimer, T. Kelly, A. Suzuki, and P.R. Subramanian, The Science Technology, and Implementation of TiAl Alloys in Commercial Aircraft Engines, *MRS Proc.*, 2013, **1516**, p 49–58. https://doi.org/10.1557/opl.2013.44
6. G.L. Chen, W.J. Zhang, Z.C. Liu, and S.J. Li, Microstructure and Properties of High-Nb contraining TiAl-base alloys, in *Gamma Titanium Aluminides 1999*. Y.W. Kim, D.M. Dimiduk, and M.H. Loretto, Eds., TMS, Warrendale, PA, 1999, p 371–380
7. V. Küstner, M. Oehring, A. Chatterjee, H. Clemens, and F. Appel, Analysis of the Solidification Microstructure of Multicomponent Gamma Titanium Aluminide Alloys, in *Solidification and Crystallization*. D.M. Herlach, Ed., John Wiley & Sons, Weinheim, 2006, p 250–259
8. J.C. Schuster, and M. Palm, Reassessment of the Binary Aluminium-Titanium Phase Diagramm, *J. Phase Equilib. Diffus.*, 2006, **27**(3), p 255–277. https://doi.org/10.1361/154770306X109809
9. S. Xu, Y. Xu, Y. Liang, X. Xu, S. Gao, Y. Wang, J. He, and J. Lin, Phase Equilibria of the Ti-Al-Nb System at 1300 °C, *J. Alloy. Compd.*, 2017, **724**, p 339–347. https://doi.org/10.1016/j.jallcom.2017.06.195
10. G.L. Chen, X.T. Wang, K.Q. Ni, S.M. Hao, J.X. Cao, J.J. Ding, and X. Zhang, Investigation on the 1000, 1150 and 1400 °C Isothermal Section of the Ti-Al-Nb System, *Intermetallics*, 1996, **4**(1), p 13–22. https://doi.org/10.1016/0966-9795(95)00012-n
11. L. Li, L. Liu, L. Zhang, L. Zeng, Y. Zhao, W. Bai, and Y. Jiang, Phase Equilibria of the Ti-Al-Nb System at 1000, 1100 and 1150 °C, *J. Phase Equilib. Diffus.*, 2018, **39**(5), p 549–561. https://doi.org/10.1007/s11669-018-0635-2
12. A. Hellwig, *Experimentalle Untersuchungen zur Konstitution des Systems Aluminium-Titan-Niob, Ph.D. thesis*, 1990, Universität Dortmund, Dortmund. p 113.
13. A. Hellwig, M. Palm, and G. Inden, Phase Equilibria in the Al-Nb-Ti System at High Temperatures, *Intermetallics*, 1998, **6**(2), p 79–94. https://doi.org/10.1016/s0966-9795(97)00043-5
14. M. Eckert, K. Hilpert, and H. Nickel, *Thermodynamische Untersuchungen zur Korrosion von binären und ternären Titanaluminiden, Bericht des FZ Jülich*, 1997. p 1-200
15. R. Kainuma, Y. Fujita, H. Mitsui, and K. Ishida, Phase Equilibria Among α (hcp), β (bcc) and γ ($L1_0$) Phases in Ti-Al Base Ternary Alloys, *Intermetallics*, 2000, **8**, p 855–867. https://doi.org/10.1016/S0966-9795(00)00015-7
16. K.J. Leonard, J.C. Mishurda, and V.K. Vasudevan, Phase Equilibria at 1100 °C in the Nb-Ti-Al System, *Mater. Sci. Eng., A*, 2002, **329–331**, p 282–288. https://doi.org/10.1016/s0921-5093(01)01567-2
17. A.M. Zakharova, G.V. Karsanov, B.S. Troitskii, and L.L. Vergasova, Isothermal Sections of the Nb-Ti-Al System at 1200-600 °C, *Izvestiya Akademii Nauk SSSR, Metally*, 1984, **1**, p 200–202.
18. U.R. Kattner, and W.J. Boettinger, Thermodynamic Calculation of the Ternary Ti-Al-Nb System, *Mater. Sci. Eng., A*, 1992, **152**(1–2), p 9–17. https://doi.org/10.1016/0921-5093(92)90039-4
19. T.J. Jewett, Comment on 'Investigation on the 1000, 1150 and 1400°C Isothermal Section of the Ti-Al-Nb System,' *Intermetallics*, 1997, **5**(2), p 157–159. https://doi.org/10.1016/s0966-9795(96)00076-3
20. J.J. Ding, and S.M. Hao, Reply to the "Comment on 'Investigation on the 1000, 1150 and 1400 °C Isothermal Section of the Ti-Al-Nb System—Part II. Modification of 1000 and 1150 °C Isothermal Sections of the Ti-Al-Nb System, *Intermetallics*, 1998, **6**(4), p 329–334.
21. G.L. Chen, J.G. Wang, X.T. Wang, X.D. Ni, S.M. Hao, and J.J. Ding, Reply to the "Comment on 'Investigation on the 1000, 1150 and 1400 °C Isothermal Section of the Ti-Al-Nb System" Part I. Ordering of Nb in γ-TiAl and γ1 Phase, *Intermetallics*, 1998, **6**(4), p 323–327. https://doi.org/10.1016/s0966-9795(97)00079-4
22. L. Tretyachenko, *Al-Nb-Ti Ternary Phase Diagram Evaluation*, in *MSI Eureka, Watson, A. (Ed.) by MSI, Materials Science International Services GmbH, Stuttgart*, 2004, Doc-ID: 10.16070.2.6
23. D.M. Cupid, O. Fabrichnaya, O. Rios, F. Ebrahimi, and H.J. Seifert, Thermodynamic Re-Assessment of the Ti-Al-Nb System, *Int. J. Mater. Res.*, 2009, **100**(2), p 218–233. https://doi.org/10.3139/146.110015
24. V.T. Witusiewicz, A.A. Bondar, U. Hecht, and T.Y. Velikanova, The Al-B-Nb-Ti System IV Experimental Study and Thermodynamic Re-Evaluation of the Binary Al-Nb and Ternary Al-Nb-Ti Systems, *J. Alloys. Compnd.*, 2009, **472**(1–2), p 133–161. https://doi.org/10.1016/j.jallcom.2008.05.008
25. M. Palm, *Al-Ti Binary Phase Diagram Evaluation*, in *MSI Eureka, Effenberg, G. (Ed.) by MSI, Materials Science International Services GmbH, Stuttgart*, 2020, Doc-ID: 20.15634.2.4.,
26. M. Takeyama, Y. Ohmura, M. Kikuchi, and T. Matsuo, Phase Equilibria and Microstructural Control of Gamma TiAl Based Alloys, *Intermetallics*, 1998, **6**(7), p 643–646. https://doi.org/10.1016/S0966-9795(98)00049-1
27. H. Nakamura, M. Takeyama, L. Wei, Y. Yamabe, and M. Kikuchi. Phase equilibira among the α, β and γ phases in the Ti-Al-X (V, Nb, Cr, Mo) systems at 1473 and 1573K. in: *3rd Japan*

International SAMPE Symposium, 1993, Chiba, 1993, p 1353-1358
28. C. Servant and I. Ansara, Thermodynamic assessment of the Al-Nb-Ti system, *Berichte der Bunsen-Gesellschaft-Physical Chemistry Chemical Physics*, 1998, **102**(9), p 1189-1205 https://doi.org/10.1002/bbpc.19981020923
29. N. Saunders, R.W. Cahn, M. McLean, M. Rappaz, and D.G. Pettifor, Phase Diagram Calculations for High-Temperature Structural Materials [and Discussion], *Philosophical Transactions: Physical Sciences and Engineering*, 1995, **351**, p 543-561 http://www.jstor.org/stable/54492
30. T. Tetsui, Effects of High Niobium Addition on the Mechanical Properties and High-Temperature Deformability of Gamma TiAl Alloy, *Intermetallics*, 2002, **10**(3), p 239–245. https://doi.org/10.1016/S0966-9795(01)00121-2
31. X.T. Wang, G.L. Chen, and K.Q. Ni, The 1400 °C Isothermal Section of the Ti-Al-Nb Ternary System, *J. Phase. Equilib.*, 1998, **19**(3), p 200–205.
32. K.J. Leonard, and V.K. Vasudevan, Phase Equilibria and Solid State Transformations in Nb-rich Nb-Ti-Al Intermetallic Alloys, *Intermetallics*, 2000, **8**(9–11), p 1257–1268. https://doi.org/10.1016/s0966-9795(00)00056-x
33. K.J. Leonard, J.C. Mishurda, and V.K. Vasudevan, Examination of Solidification Pathways and the Liquidus Surface in the Nb-Ti-Al System, *Metall. Mater. Trans. B.*, 2000, **6**, p 1305–1321.
34. B. Distl, K. Hauschildt, B. Rashkova, F. Pyczak, and F. Stein, Phase Equilibria in the Ti-Rich Part of the Ti-Al-Nb System—Part I: Low-Temperature Phase Equilibria Between 700 and 900 °C, *J. Phase. Equilib. Diffus.*, 2022, **43**(3), p 355–381.
35. R. Kainuma, M. Palm, and G. Inden, Solid-Phase Equilibria in the Ti-rich Part of the Ti-Al System, *Intermetallics*, 1994, **2**(4), p 321–332. https://doi.org/10.1016/0966-9795(94)90018-3
36. L.S. T'sai, and T.R. Hogness, The Diffusion of Gases Through Fused Quartz, *J. Phys. Chem.*, 1932, **36**(10), p 2595–2600. https://doi.org/10.1021/j150340a007
37. X. Llovet, A. Moy, P.T. Pinard, and J.H. Fournelle, Electron Probe Microanalysis: A Review of Recent Developments and Applications in Materials Science and Engineering, *Prog. Mater Sci.*, 2021, **116**, p 100673. https://doi.org/10.1016/j.pmatsci.2020.100673
38. B. Distl, K. Hauschildt, F. Pyczak, and F. Stein, Solid-Solid Phase Transformations and Their Kinetics in Ti-Al-Nb Alloys, *Metals.*, 2021, **11**(12), p 1991.
39. H. Okamoto, Nb-Ti (Niobium-Titanium), *J. Phase. Equilib.*, 2002, **23**(6), p 553–553. https://doi.org/10.1361/105497102770331325
40. L.A. Bendersky, W.J. Boettinger, B.P. Burton, F.S. Biancaniello, and C.B. Shoemaker, The Formation of Ordered ω-Related Phases in Alloys of Composition Ti_4Al_3Nb, *Acta. Metall. Mater.*, 1990, **38**(6), p 931–943. https://doi.org/10.1016/0956-7151(90)90165-D
41. L.A. Bendersky, B.P. Burton, W.J. Boettinger, and F.S. Biancaniello, Ordered Omega-Derivatives in a Ti-37.5Al-20Nb at.% Alloy, *Scripta. Metall. et Mater.*, 1990, **24**, p 1541–1546. https://doi.org/10.1016/0956-716X(90)90429-K
42. M. Takeyama, and M. Kikuchi, Phase Equilibria and Microstructure Evolution of Gamma Titanium Aluminides-Effect of Third Alloying Element on Binary Ti-Al Alloys, *Materia. Japan.*, 1996, **35**, p 1058–1061.
43. B. Distl, G. Dehm, and F. Stein, Effect of Oxygen on High-temperature Phase Equilibria in Ternary Ti-Al-Nb Alloys, *Z. Anorg. Allg. Chem.*, 2020, **646**(14), p 1151–1156. https://doi.org/10.1002/zaac.202000098
44. H.F. Chladil, H. Clemens, G.A. Zickler, M. Takeyama, E. Kozeschnik, A. Bartels, T. Buslaps, R. Gerling, S. Kremmer, L. Yeoh, and K.-D. Liss, Experimental Studies and Thermodynamic Simulation of Phase Transformations in High Nb Containing γ-TiAl Based Alloys, *Int. J. Mater. Res.*, 2007, **98**(11), p 1131–1137. https://doi.org/10.3139/146.101569
45. H.F. Chladil, H. Clemens, H. Leitner, A. Bartels, R. Gerling, F.P. Schimansky, and S. Kremmer, Phase Transformations in High Niobium and Carbon Containing γ-TiAl Based Alloys, *Intermetallics*, 2006, **14**(10), p 1194–1198. https://doi.org/10.1016/j.intermet.2005.11.016
46. K.-D. Liss, A. Bartels, H. Clemens, S. Bystrzanowski, A. Stark, T. Buslaps, F.-P. Schimansky, R. Gerling, C. Scheu, and A. Schreyer, Recrystallization and Phase Transitions in a γ-TiAl-Based Alloy as Observed by ex Situ and in Situ High-Energy x-ray Diffraction, *Acta. Mater.*, 2006, **54**(14), p 3721–3735. https://doi.org/10.1016/j.actamat.2006.04.004
47. L.A. Yeoh, K.-D. Liss, A. Bartels, H. Chladil, M. Avdeev, H. Clemens, R. Gerling, and T. Buslaps, In Situ High-Energy x-ray Diffraction Study and Quantitative Phase Analysis in the $\alpha + \gamma$ Phase Field of Titanium Aluminides, *Scripta. Mater.*, 2007, **57**(12), p 1145–1148. https://doi.org/10.1016/j.scriptamat.2007.08.021
48. E. Scheil, Darstellung von Dreistoffsystemen, *Archiv für das Eisenhüttenwesen*, 1936, **9**(11), p 571–573. https://doi.org/10.1002/srin.193600784
49. C. He, F. Stein, and M. Palm, Thermodynamic Description of the Systems Co-Nb, Al-Nb and Co-Al-Nb, *J. Alloy. Compd.*, 2015, **637**, p 361–375. https://doi.org/10.1016/j.jallcom.2015.02.182
50. J. Braun, and M. Ellner, x-ray High-Temperature In Situ Investigation of the Aluminide $TiAl_2$ ($HfGa_2$ type), *J. Alloy. Compd.*, 2000, **309**(1), p 118–122. https://doi.org/10.1016/S0925-8388(00)01031-8
51. J. Braun, and M. Ellner, Phase Equilibria Investigations on the Aluminium-Richt Part of the Binary System Ti-Al, *Metall. Mater. Trans. A.*, 2001, **32**(5), p 1037–1047. https://doi.org/10.1007/s11661-001-0114-x
52. V. Witusiewicz, A. Bondar, U. Hecht, O. Stryzhyboroda, N. Tsyganenko, V. Voblikov, V. Petyukh, and T.Y. Velikanova, Thermodynamic Re-Modelling of the Ternary Al-Mo-Ti System Based on Novel Experimental Data, *J. Alloy. Compd.*, 2018, **749**, p 1071–1091. https://doi.org/10.1016/j.jallcom.2018.03.283
53. A. Shaaban, L.J. Signori, H. Nakashima, and M. Takeyama, Effects of the Addition of Transition Metals on Phase Equilibria and Phase Transformations in TiAl Systems in Between 1473 and 1073 K, *J. Alloy. Compd.*, 2021, **878**, p 160392. https://doi.org/10.1016/j.jallcom.2021.160392